UNIVERSIDAD DE CHILE

FACULTAD DE CIENCIAS QUÍMICAS Y FARMACÉUTICAS

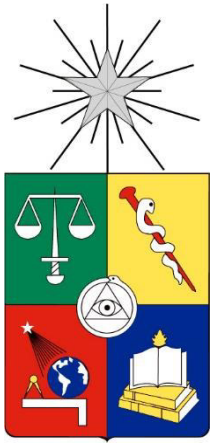

Studying the role of BiP as a chaperone through single molecule force spectroscopy.

Tesis presentada a la Universidad de Chile para optar al grado de Magíster en Bioquímica área de Especialización en Proteínas Recombinantes y Biotecnología y Memoria para optar al Título de Bioquímico por:

MARÍA PAZ RAMÍREZ LÓPEZ

Directores de Tesis: Dr. Christian AM Wilson y Dr. Elias Puchner

Santiago-CHILE diciembre 2016

UNIVERSIDAD DE CHILE
FACULTAD DE CIENCIAS QUÍMICAS Y FARMACÉUTICAS

INFORME DE APROBACIÓN DE TESIS

Se informa a la Dirección de la Escuela de Graduados de la Facultad de Ciencias Químicas y Farmacéuticas que la Tesis de Magíster y Memoria de Título presentada por la candidata

MARÍA PAZ RAMÍREZ LÓPEZ

Ha sido aprobada por la Comisión de Evaluadora de Tesis como requisito para optar al grado de Magíster en Bioquímica, Área de Especialización en Proteínas Recombinantes y Biotecnología y Título de Bioquímica, en el examen público rendido el día

_____

Directores de Tesis:
Dr. Christian A.M. Wilson
Dr. Elias Puchner

_____

Comisión Evaluadora de Tesis:

Dr. Mauricio Baez Larach

_____

Dr. María Antonieta Valenzuela

_____

Dr. Francisco Melo _____

Lugar de desarrollo de la tesis:

Laboratorio de Bioquímica, Facultad de Ciencias Químicas y Farmacéuticas, Universidad de Chile, Santiago de Chile

Laboratory of Cellular and Molecular Biophysics, School of Physics & Astronomy, University of Minnesota Laboratory of Cellular and Molecular Biophysics, School of Physics & Astronomy, University of Minnesota.

Financiamiento:

Proyecto Fondecyt iniciación Chile, código: 11130263

Programa de colaboración internacional CONICYT PCI: PII20150073

Beca CONICYT magister Nacional 2015**, Folio:** 22151448

Vicerrectoría de Asuntos Académicos Universidad de Chile: Ayudas para Estadías Cortas de Investigación

INDEX

FIGURES INDEX

TABLE INDEX

ABBREVIATIONS

°C	Celsius degrees
Aa	Aminoacid
AND	Deoxyribonucleic acid
ADP	Adenosine 5’ diphosphate
App	Apparent
ATP	Adenosine 5’ triphosphate
Bp	Base pair
BSA	Bovine serum albumin
C-terminus	Carboxy terminus
D.R	Disappearance of refolding rip
dNTP	Deoxyribonucleotides
Ds	Double stranded
DTT	Dithiotreitrol
G6PDH	Glucose-6-phosphate dehydrogenase
His	Histidine
IPTG	Isopropyl β-D-1-thiogalactopyranoside
Kb	Kilo base
kDa	Kilo Dalton
Min	Minute
mM	Millimolar
NAD^+	Nicotinamide
NBD	Nucleotide Binding Domain
NBT	Nitro blue tetrazolium
Nm	Nanometer
N-terminus	Amino terminus
OD	Optical density
Pi	Inorganic phosphate
PCR	Polymerase chain reaction
PEG	Polyethylene glycol

PMS	Phenazine methosulfate
PSD	Position sensitive detector
Rpm	Revolution per minute
RT	Room temperature
R.U	Reappearance of unfolding rip
SBD	Substrate Binding Domain
SDS	Sodium dodecyl sulfate
TBS	Tris-Buffered Saline
tlGK	Glucokinase from *Thermococcus litoralis*
WLC	Worm like chain
µM	Micromolar

ABSTRACT

Studying the role of BiP as a chaperone through single molecule force spectroscopy.

Quality control and proteostasis are crucial processes in the cell to maintain homeostasis, and chaperones have a key role in this. BiP (Immunoglobulin Binding Protein) is an ER-located (Endoplasmic Reticulum) member of the family of HSP70 molecular chaperones that participates is various processes, such as protein folding and activation of the unfolded protein response. BiP binds to proteins and stabilizes their unfolded state, then unbinds to give them a chance to spontaneously fold. If proteins are unable to do so BiP binds once more, avoiding misfolding and aggregation.

The aim of this project was to study the function of BiP as a chaperone. It was unknown how BiP exactly affected the protein folding pathway and it had not been directly demonstrated to which folding state of the substrate protein it binds. In addition, to our knowledge all studies regarding BiP binding and affinity have been done using peptides and not full proteins. For this, optical tweezers for single molecule force spectroscopy experiments were employed to investigate how BiP affects the folding mechanism of a protein and how this effect depends on nucleotides.

Using the protein MJ0366 as BiP's substrate, which most likely has just one binding site, pulling and relaxing cycles at constant velocity to unfold and refold the protein substrate were performed. In the absence of BiP, MJ0366 unfolded and refolded in every pulling cycle. However, when BiP was added the frequency of folding events of MJ0366 significantly decreased. The loss in folding always occurred after a successful unfolding event.

This process was dependent on ATP and ADP concentrations, since when either ATP was decreased or ADP was added, the duration of periods without folding events increased. The observed effect was due to the binding of BiP to MJ0366 and not nonspecific interactions (BSA or lysozyme, used as controls). These results show that the affinity for the substrate

protein increased in these conditions. Therefore, we conclude that BiP binds to the unfolded state of MJ0366 and prevents its refolding and that this effect depends on the type and concentration of nucleotides.

In summary, BiP chaperone binding/release has a very clear effect in protein folding, after mechanical unfolding of the protein MJ0366 BiP is able to find its binding site, or sites (the number of binding sites has not been experimentally demonstrated in this work), and bind in a reversible manner, avoiding the formation of tertiary contacts. Future studies will be performed with different concentrations of BiP to confirm that there is only one binding site for BiP in MJ0366 and so, empirically validate our model and calculated affinity constants.

RESUMEN

Estudiando el rol chaperona de BiP a través de la espectroscopía de fuerza a nivel de molécula única.

El control de calidad y la *proteostasis* son procesos cruciales en la célula para mantener la homeostasis, y las chaperonas tienen un rol clave en esto. BiP (Por sus siglas in inglés Immunoglobulin Binding Protein) es un miembro de la familia de chaperonas moleculares HSP70 localizada en el Retículo endoplásmico que participa en varios procesos, tales como el plegamiento de proteínas y la activación de la respuesta de proteínas desplegadas, UPR (por sus siglas en inglés Unfolded Protein Response). BiP se une a las proteínas y estabiliza su estado desplegado, luego se desune para darles la oportunidad de plegarse espontáneamente. Si las proteínas son incapaces de hacerlo BiP se une una vez más, evitando así el plegamiento erróneo y la agregación.

El objetivo de este proyecto fue estudiar la función de BiP como chaperona. Se desconocía cómo BiP afectaba exactamente a las vías de plegamiento de las proteínas y no se había demostrado directamente a qué estado de plegamiento de la proteína de sustrato se une. Además, a nuestro conocimiento todos los estudios sobre la unión de BiP y afinidad se han hecho utilizando péptidos y no proteínas completas. Para este estudio se emplearon pinzas ópticas para experimentos de espectroscopía de fuerza de molécula única para investigar cómo BiP afecta al mecanismo de plegamiento de una proteína y cómo este efecto depende de los nucleótidos.

Usando la proteína MJ0366 como sustrato de BiP, se realizaron ciclos de estiramiento y relajación a velocidad constante para desplegar y replegar el sustrato la proteína sustrato. En ausencia de BiP, MJ0366 se desplegó y se replegó en cada ciclo de tiraje. Sin embargo, cuando se añadió BiP, la frecuencia de los eventos de plegamiento de MJ0366 disminuyó significativamente. La pérdida de estos eventos siempre ocurrió después de un evento de despliegue exitoso.

Este proceso fue dependiente de las concentraciones de ATP y ADP, cuando se disminuyó el ATP o se añadió ADP, aumentó la duración de los períodos sin eventos de plegamiento. El efecto observado se debió a la unión de BiP a MJ0366 y no a interacciones inespecíficas (BSA o lisozima, usados como control). Estos resultados muestran que la afinidad por la proteína sustrato aumentó en estas condiciones. Por lo tanto, concluimos que BiP se une al estado desplegado de MJ0366 evitando su replegamiento y que este efecto depende del tipo y concentración de nucleótidos.

En resumen, la unión / liberación de la chaperona BiP tiene un efecto muy claro en el plegamiento de proteínas, después del despliegue mecánico de la proteína MJ0366 BiP es capaz de encontrar su sitio de unión, o sitios de unión (el número de sitios de unión no se ha demostrado experimentalmente en este trabajo), y unirse a ella de manera reversible, evitando la formación de contactos terciarios. Futuros estudios se llevarán a cabo con diferentes concentraciones de BiP para confirmar que sólo hay un sitio de unión para BiP en MJ0366 y así, empíricamente validar nuestro modelo y constantes de afinidad calculadas.

1. INTRODUCTION

Proteins are one of the principal functional unit of the cell. They are complex biological macromolecules involved in almost every biological process. To be able to function, the nascent linear amino acid sequence of the polypeptide chain must fold correctly to its three-dimensional conformation[1]. Proteins must be able to fold and maintain this folding in the cellular environment, which is highly crowded and prone to aberrant interactions that can lead to misfolding and aggregation[2,3]. These aberrant interactions can also be induced by external environmental factors that lead to an increase in the load of proteins[4]. Degenerative diseases such as Alzheimer and Parkinson disease are caused by aggregation and accumulation of misfolded proteins[5], for this reason protein misfolding is a very relevant topic in biology and medicine. To maintain proteome homeostasis, the cell employs a variety of coordinated strategies to regulate their synthesis, folding and turnover. The cellular machinery that carries out this mission is very diverse, which includes several types of proteins [6], one of the most prominent, the molecular chaperones. These are defined as any protein that stabilizes or helps another protein to acquire its functionally active conformation, without being present in the client protein final structure[7]. Quality control and *proteostasis* are crucial in maintaining cellular homeostasis, and the chaperones have a key role in this. They assist in different processes, like *de novo* folding or refolding, the unfolded protein response (UPR), the ubiquitin-proteasome system (UPS) and autophagy, among others[3,5,8].

1.1 BiP chaperone

Several classes of structurally different but functionally related chaperones exist in cells, forming cooperative pathways and networks in order to maintain proteostasis[2]. These chaperones can be classified by their dependence and independence on ATP. ATP-dependent chaperons rely on cycles of ATP hydrolysis to drive the binding and release of their client proteins, whereas the latter are “holdases” that keep the protein unfolded and unable to interact and aggregate. In this case the energy dependent step is performed by another chaperone[3,9]. From the several types of chaperones in the cell, the HSP70 family is a group of conserved chaperones with ATPase activity that is essentially involved in protein folding[10]. This group of chaperones is present in prokaryotes, eukaryotes, and archaea and exhibits conservation in its action mechanism[11]. One of the most extensively studied

members of the HSP70 family is the Immunoglobulin Binding Protein (BiP, Kar2p in yeast). BiP resides inside the endoplasmic reticulum (ER) and is considered to be the master regulator of the ER[12,13]. This chaperone plays a role in assisting protein translocation into the ER, by binding to nascent proteins, in participating in the activation of the IRE1 pathway in the unfolded protein response (UPR) and in the retrograde transport of aberrant proteins destined for proteasome dependent degradation across the ER membrane[14,15].

BiP has two domains, an N-terminal ATPase domain, known as nucleotide binding domain (NBD), and a C-terminal substrate binding domain (SBD) (Fig. 1). The NBD, hydrolyzes ATP to ADP and Pi and the SBD, binds to polypeptides with diverse sequences allowing BiP to interact with a wide variety of unrelated nascent polypeptides. In particular, it binds to a heptameric motif, Hy(WX)HyXHyXHy, where Hy is a bulky aromatic or hydrophobic residue, W is tryptophan, and X is any amino acid[16]. The SBD has two subdomains, α and β. The β subdomain has the binding pocket for polypeptides and the α subdomain acts as a lid that covers it[17]. BiP's activity depends on an ATPase cycle, where ATP binding regulates the affinity and kinetics of substrate binding to the SBD. When ATP is bound to BiP, the lid is open and decreases the affinity for the substrate peptide. However, when ATP is hydrolyzed to ADP the lid closes, which results in an increased affinity for the polypeptide (Fig. 2)[18,19]. The exchange of ADP to ATP finally leads to the peptide's release [18].

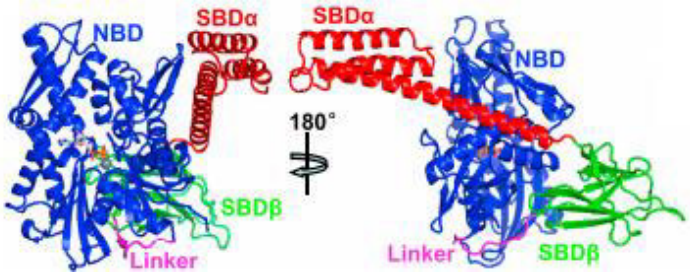

Figure 1. Structure of ATP-Bound BiP in the Open Conformation. BiP has two domains, the NBD (blue) and the SBD, which has two subdomains, α (red) and β (green). The first one acts as an α helix lid that covers the binding pocket for polypeptides formed by β sheets. In the ATP bound conformation the lid is open. The linker between the domains is in pink. Modified from Yang et al. (2015)[20].

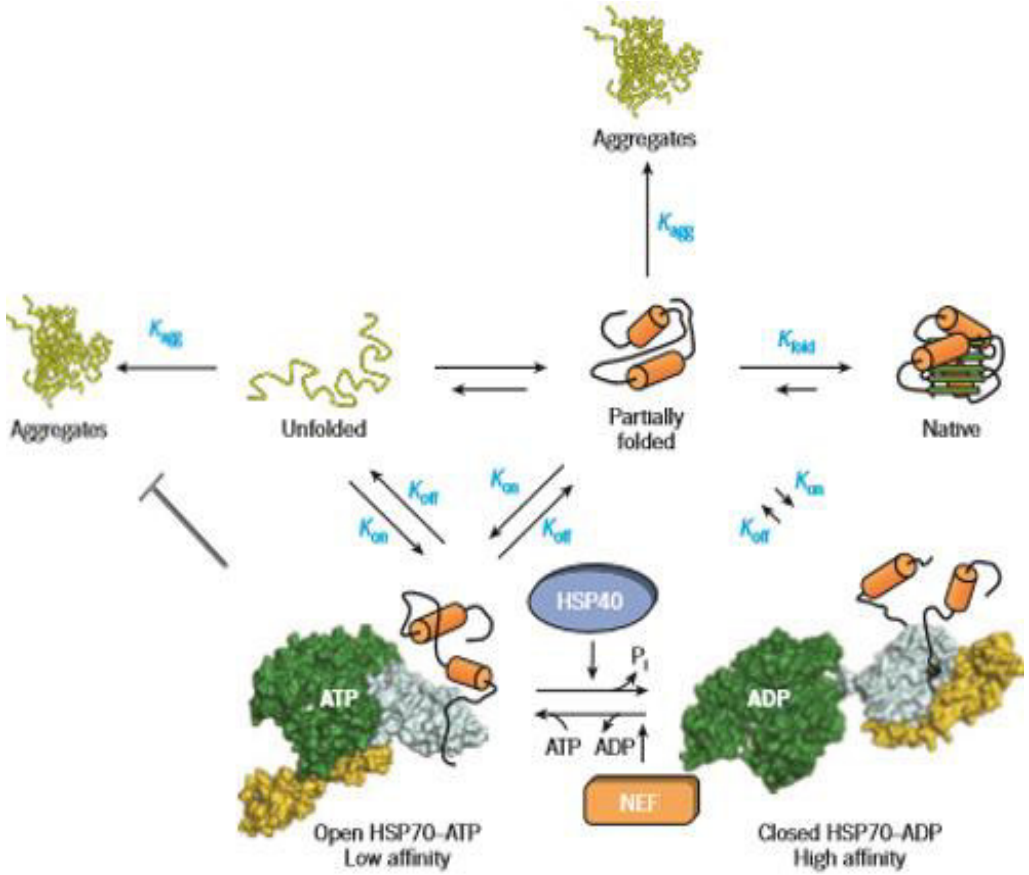

Figure 2. The HSP70 chaperone allosteric cycle and protein folding. HSP70 can be switched between high- and low-affinity states for unfolded and partially folded protein by ATP binding and hydrolysis. Unfolded and partially folded substrates, exposing hydrophobic motifs are recognized by ATP-bound HSP70. ATP hydrolysis, accelerated by HSP40 cofactor and/or the substrate binding, leads to lid closure and tight binding of substrate. Release of ADP, promoted by one of several nucleotide-exchange factors (NEFs) is required for recycling. Opening of the lid, induced by ATP binding, results in substrate release. Modified from Hartl (2011)[2].

1.2 Proteostasis and molecular chaperone BiP

The number of possible conformations that a protein chain can adopt is very large. The current model proposes that polypeptide chains explore a funnel-shaped potential energy landscape as they progress, through structural intermediates, towards their native structure[2,21,22]. Their paths to this can be minimally frustrated or be rugged. Because of this ruggedness trapped species may form as partially folded states become transiently populated (Fig. 3)[2,21]. Partially folded or misfolded states often tend to aggregate, particularly when they represent major kinetic traps in the folding pathway[23]. This can lead to amorphous structures or highly ordered, fibrillar aggregates called amyloid (Fig. 3). To avoid this and ensure efficient folding, chaperones bind to hydrophobic regions of a non-native protein transiently to blocks aggregation[8]. ATP-triggered release allows folding to proceed by letting fast-folding polypeptides collapse and bury their non-polar residues, whereas slower folding molecules that need longer than a few seconds, or failure to reach the correctly folded state leads to re-binding, in this way avoiding aggregation by stabilizing the unfolded state until they can spontaneously fold[2,5,24]. However, there are proteins that have such a frustrated folding pathway that without the assistance of chaperones simply cannot fold[25].

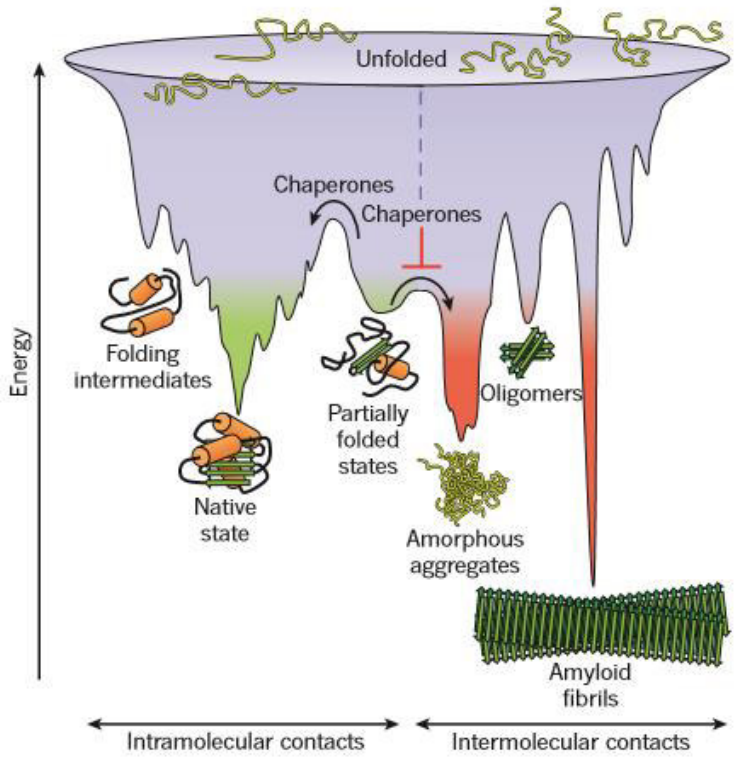

Figure 3. Different competing folding and aggregation states. Scheme of the funnel-shaped free-energy surface that proteins explore as they move towards lowest energy conformation, the native state (green minimum). The ruggedness of the landscape may result in the accumulation of kinetically trapped conformations. Chaperones may increase the efficiency and accelerate these steps *in vivo*. When several molecules fold simultaneously in a crowded environment, frustrated interactions may occur, leading to intermolecular aggregation, resulting in the formation of amorphous aggregates, toxic oligomers or ordered amyloid fibrils (red minimums). It may initiate from intermediates populated during *de novo* folding or after destabilization of the native state, and is normally prevented by molecular chaperones. Modified from Hartl (2011)[2].

1.3 Single molecule force spectroscopy: Optical tweezers.

Despite the key role of BiP as a chaperone, some important features including the binding mechanism to its substrate still remain unknown. Although structural and functional studies throughout the years revealed valuable information about where BiP binds and how it affects protein folding pathways, it has not been directly demonstrated yet whether BiP binds to folded or to unfolded protein substrates. Since BiP recognizes linear motifs enriched in hydrophobic residues[16], due to their hydrophobic nature, are most likely located in the interior of a folded protein, and because BiP interacts with early and less compactly folded intermediates[26], it has been proposed that BiP binds to the unfolded state of proteins. But no direct observation has been carried out so far, which is partially due to the experimental challenge to prepare protein substrates that can be driven to an unfolded state in a controlled and non-interfering way. In addition, to our knowledge all studies regarding BiP binding and affinity have been done using peptides and not complete proteins. Most investigations on the mechanism of the BiP chaperone are based on bulk experiments, which often mask the heterogeneity inherent to the populations of macromolecules. Given the global effect of denaturing methods and agents, it would be very difficult to study the effect of chaperones in unfolded substrates, as both would most likely unfold in such conditions. Single molecule approaches, especially single molecule force spectroscopy experiments, thus present an ideal approach to study the mechanism of BiP as they act as a local and controlled denaturing method[27] allowing for both, reversibly driving a protein substrate to an unfolded state and detecting the binding and folding events of individual proteins. The principle for the optical tweezers technique is optical trapping of particles by a potential well formed by near-infrared light. In this trap, the particle experiences force if it is displaced from the center of the trap. This allows us to manipulate individual molecules with nanometer accuracy, and also to measure the forces in the piconewton range generated during different biological processes[6]. The manipulation experiments are done by attaching double strand DNA handles to specific points of the protein through a disulfide bond (Fig. 5, shown later)[28]. In this way it is possible to pull and apply force to the protein from different chosen axes.

1.4 Chaperone studies at single molecule level.

Studies of HSP70 family members using single molecule smFRET (single molecule Förster Resonance Energy Transfer), for instance, have shown interesting results of the conformational changes occurring in the yeast Kar2 chaperone upon binding different nucleotides[29]. A different study by Bechtluft et al.[30], using optical tweezers showed a clear effect on the folding of the maltose binding protein upon binding of the chaperone SecB. It was shown that SecB binds to the unfolded protein and prevents it from complete refolding (Fig. 4). Therefore, employing these modern optical tweezers tools is useful to study the operating mechanism of these molecular machines and will allow us to directly probe changes in folding the mechanism of a substrate protein in the presence and absence of BiP.

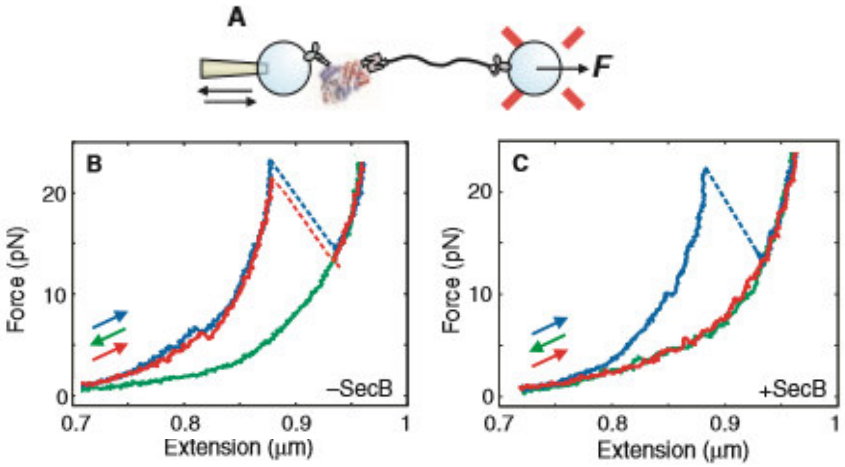

Figure 4. Experimental setup and MBP force-extension curves. A. MBP is tethered between two beads, one held by a micropipette, the other by an optical trap that allows force detection. At the C terminus MBP is attached to the bead using an antibody that recognized a myc-tag. The N terminus it is attached via streptavidin-biotin linkages to a DNA handle, which in turn is attached to the bead surface through an antibody that recognized digoxigenin. **B.** Force-extension curves in the absence of SecB showing unfolding at high force (blue), refolding at low forces (green), and again unfolding at high force (red). **C.** Force-extension curves in the presence of SecB (0.1 mM). The second stretching curve (red) lacks the typical unfolding features, being the same as the refolding curve, showing that stable tertiary interactions are absent. Modified from Bechtluft et al. (2007)[30].

1.5 Experimental model: MJ0366 protein.

For this study single molecule force spectroscopy with optical tweezers is employed to study BiP's function as a chaperone and to determine how it affects protein folding *in singulo*. The substrate protein selected for BiP was the well characterized[31] protein MJ0366, a hypothetical cell-expressed knotted protein from *Methanocaldococcus jannaschii*, which was used for various reasons. First, MJ0366 was found to be easily modified with DNA handles for optical tweezers experiments. Second, its mechanical unfolding and refolding behavior has been well characterized in our lab at single molecule level [Doctoral Thesis of Maira Rivera, PhD student at the laboratory of Mauricio Baez] and exhibits clearly detectable folding and unfolding events, which is crucial for this study. Third, MJ0366 has most likely just one putative binding site for BiP allowing a simpler analysis and interpretation of data.

2. HYPOTHESIS

BiP, in its chaperone function, will bind to the unfolded state of proteins by hindering the formation of tertiary contacts.

3. OBJETIVES

3.1. General Objective:

To determine the effect of BiP binding/release on protein folding. In particular, its function as chaperon and how it interacts with its substrate.

3.2. Specific Objectives:

3.2.1 To determine which protein folding state BiP binds to.

3.2.2 To determine the effect of the type and concentration of nucleotide on BiP's binding affinity and kinetics.

4. MATERIALS AND METHODS

4.1. Materials

Reactive	Brand	Catalog number
Acetic Acid	Merck	1.00063.2500
Acrilamyde	Invitrogen	15512-023
Agar-Agar	Merck	1.01614.1000
Ampicillin	Sigma	A0166
ATP	GoldBio	A-081-5
BSA	Sigma	A-4503
β-Mercaptoethanol	Sigma	M6250
Bradford Reactive	Bio-Rad	500-0006
Calcium chloride	Merck	2381
Coomassie Brilliant blue R250	Merck	1.12553.0025
dNTP	KAPA	KN1002-5
DTT	Promega	V3151
Glucose	Merck	8342
G6PDH	Sigma	G-6378
Glycerol (85%)	Merck	1.04094.1000
Glycine	Merck	1.2008.1000
HEPES	Sigma	H4034
Hydrogen chloride (32%)	Merck	1.00317.2500
Imidazole	USBiological	C7030931
IPTG	Bioline	BIO-37036
LB Broth growth medium	MO BIO	12106-1
Lyzozyme	Sigma	L6876
Magnesium Acetate	Sigma	M0631
Magnesium Chloride	Merck	1.05833.1000
Methanol	Merck	1.06009.2500
NBT	GoldBio	298-83-9
Page Ruler Prestained Protein Ladder	Thermo Scientific	26616
Pepstatin	Sigma	P5318
Peptone	BD	211677
PMSF	Sigma Aldrich	78830
Potassium Chloride	BDH	29594
SDS	Merck	428015
Sodium Chroride	Merck	1.06404.1000
Tris base	Merck	1.08382.0500
Triton X-100	Sigma	X100-1L
Tween20	US Biological	P4379

4.2. Methods

4.2.1 BiP expression and purification. The RR1 *Escherichia coli* strain, containing the pMR2623[32] expression plasmid for BiP with an N-terminal fusion to a His-tag, was kindly provided by Jeffrey Brodsky (Pittsburgh University). Purified BiP was obtained from cultures of RR1 *E. coli* cells grown in Luria Broth (LB) media supplemented with 100 μg/ml ampicillin as a selection marker, at 26°C with a constant agitation of 230 rpm.

A 50 mL overnight culture was inoculated into 1 L of LB-ampicillin media and incubated until the culture reached an OD_{600}=0.6. After this, to induce overexpression of the protein construct, IPTG was added to a final concentration of 0.5 mM and the incubation continued for another 4 hours. The induced bacteria were harvested by centrifugation for 15 min at 10,000 rpm at 4 °C using a Sorvall RC-5B centrifuge with a GSA rotor. For protein purification, cells were resuspended and washed once in water, harvested again in the same conditions and the final bacteria pellet was frozen at -20 °C until further use.

BiP was purified by combining and modifying two previously published protocols of two affinity chromatographies, a nickel affinity and an ATP-agarose affinity one, in order to obtain BiP in purer and in higher yield. First a nickel affinity column purification[33] was used, followed by a 5 ml ATP-agarose affinity column purification[34]. In detail, purification of BiP was started by thawing the pellet and resuspending it in 15 mL of fresh sonication buffer (50 mM HEPES, pH 7.4, 300 mM NaCl, 10 mM imidazole, 5 mM β-mercaptoethanol) and adding 1 mM of PMSF, leupeptin and pepstatin each. The bacteria suspension was lysed in ice by sonication at 40% power 50% of rest time for 8 min (Sonic ruptor 250, Omni international) and the cell debris and supernatant were separated by centrifugation at 10,000 rpm for 15 min at 4 °C using a Sorvall SS-34 rotor. The supernatant was loaded onto a prepacked a 1 mL His Trap HP (General Electric), previously equilibrated with 10 volumes of sonication buffer, at a loading rate of 1mL/min. The flow through was collected and an initial wash with 15 volumes of sonication buffer was performed. After this, 5 sequential wash steps, done with 15 volumes of buffer each (wash buffer 1 to 5), were performed to eliminate any additional proteins that may interact with the column. The composition of the wash buffers were as following; Wash buffer 1: sonication buffer + 1% Triton X-100 + 5% glycerol; Wash buffer 2: sonication buffer + 1M NaCl + 5% glycerol; Wash buffer 3:

sonication buffer + 5 mM ATP; Wash buffer 4: sonication buffer + 0.5M Tris, pH 7.4; Wash buffer 5: sonication buffer + 25 mM imidazole + 5% glycerol. All wash eluted fractions were collected. Finally, BiP protein was eluted with a 30 ml by 30 ml gradient of elution buffer sonication buffer + 5% glycerol + 25 mM imidazole and elution buffer with 250 mM imidazole, 1 mL fractions were collected. All collected fractions (flow through, washes and eluted fractions) were assessed by a 10% acrylamide gel electrophoresis in denaturating conditions in the presence of SDS (SDS-PAGE). The gel was loaded with 15 µL using 4X loading buffer (Laemmli). The gel was run using running buffer (25 mM Tris, 190 mM glycine and 0.1% SDS) at constant voltage, 100 volts. The gel was then stained with R-250 Coomasie blue and destained with a 10% acetic acid solution.

The eluted fractions that contained purified BiP were pooled together and loaded into a 5 mL self-packed degassed ATP-agarose column (sigma) previously equilibrated with 4 volumes Buffer C (20 mM HEPES pH 7, 25 mM KCl, 2 mM MgOAc, 0.8 mM DTT), at a loading rate of 0.4 mL/min. This purification step was to further purify and to discard inactive BiP, which doesn't bind to the column due to lack of its ATPase activity. After this, 3 sequential wash steps of 4 volumes each were performed at a flow rate of 0.8 mL/min, a first wash with buffer C, a second one with buffer C + 1 M KCl to eliminate nonspecific interactions and a third with buffer C to remove the KCl. Finally, BiP was eluted with Buffer C supplemented with 2 mM ATP, fractions of 1 mL were collected and the presence of purified protein in the fractions were assessed by Bradford's method[35], using BSA as standard. All fractions collected (flow through, washes and pooled eluted fractions that contained protein) were again assessed by a 10% SDS-PAGE in the same conditions. The final purified product was snap-frozen in liquid nitrogen and stored at -80 °C for later use.

4.2.2 Western blot analysis. A total of 15 µg of protein was loaded onto an 8% SDS-PAGE gel and run in running buffer at 100 V for 2 h. Proteins were then transferred onto a PVDF membrane using transfer buffer (25 mM Tris, 190 mM glycine and 20% methanol) for 2 h at 100 V. After completing transference, membranes were blocked using TBS + 0.1% Tween20 containing 5% milk for 60 min at RT, then probed overnight with anti-Kar2 primary antibody, kindly provided by Randy Schekman Lab's (UC Berkeley), diluted in the blocking solution 1:10,000 at 4 °C with agitation. Next day the membranes where washed 3 times, for

five minutes each wash, with TBS + 0.1% Tween20 and incubated for 2 hours at RT with an anti-rabbit secondary antibody (Invitrogen) diluted in the blocking solution 1:3,000. Bound antibodies were detected with peroxidase-coupled assay using an ECL™ western blotting analysis system with a 10 sec exposure.

4.2.3 ATPase assay. To measure the activity of purified BiP a spectrophotometrical coupled assay was performed measuring the formation of a formazan blue precipitate[36]. The assay consists in coupling the formation of ADP, produced ATPase activity of BiP, to the production of glucose-6-phosphate by *Thermococcus litoralis* glucokinase[37], then the reduction of NAD^+ by glucose 6 phosphate dehydrogenase (Sigma), then the reduction of PMS and finally the formation of formazan.

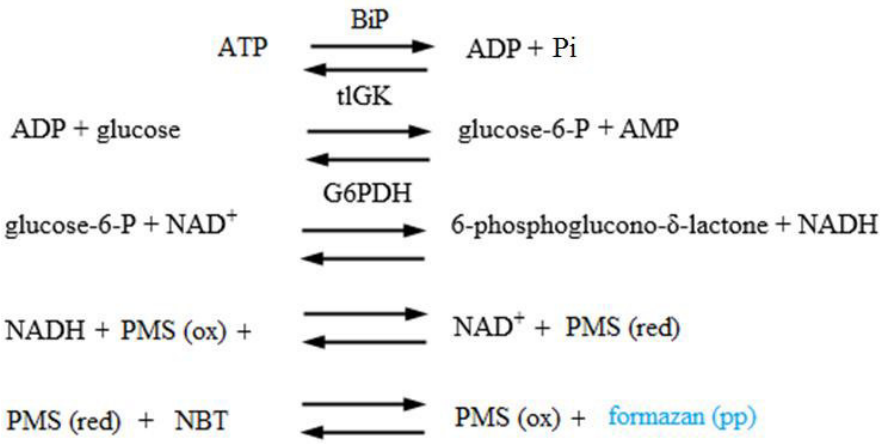

The reaction buffer contained 100 mM HEPES pH 7.0, 2 mM ATP, 1mM NAD, 7 mM $MgCl_2$, 9 mM glucose, 25 mM KCl, 0.5 mM DTT, 0.2 mM NBT, 0.4 mM PMS, 10 U *Thermococcus litoralis* glucokinase and 25 U glucose 6 phosphate dehydrogenase. The reaction was started by addition of the BiP enzyme solution to a final concentration of 4 µM and then left at RT in darkness for 1 hour. After this time the reaction was terminated by the addition of 2 volumes of 0.1 M HCl. The formazan product was determined by the change in absorbance at 550 nm, $\varepsilon_{formazan}$= 0.795 $mM^{-1}cm^{-1}$. A non-enzymatic control was also performed, where instead of BiP buffer was added in the same amount. One unit of enzyme activity was defined as in Koga et al, as the amount of enzyme required to convert 1 µmol of glucose per min[36].

4.2.4 Preparation of MJ0366 samples for optical tweezers. The electroeluted and purified DNA-MJ0366-DNA construct, kindly provided by Maira Rivera[28,38], was first incubated with 3.10 µm anti-digoxigenin coated polystyrene beads (dig-beads) for 15 min at RT. After this time the optical tweezers buffer (20 mM HEPES pH 7.0, 2 mM ATP, 2 mM $MgCl_2$, 15 mM Na_2HPO_4 pH 7.6, 0.1 mM EDTA, 25 mM KCl, 0.5 mM DTT) was added to a final volume of 500 µL. The used dilution of the DNA-MJ0366-DNA constructs was optimized to yield the best density for performing optical tweezers experiments. Finally, this solution was injected into the optical tweezers chamber and a DNA-MJ0366-DNA construct bound to a dig-bead was placed in the optical trap and then brought in close proximity to a 2.10 µm streptavidin-coated bead (Spherotech) which was held in place at the end of a pipette by suction, until a tether between the two beads was attained[28]. Dig-beads were generated by coupling anti-digoxigenin antibodies (Roche) to 3.2 µm proteinG-coated beads (Spherotech)[28].

4.2.5 Optical tweezers experiments. The pulling experiments at a constant velocity were performed using a simple trap optical tweezers instrument, called "miniTweezers"[39]. It is an analytical optical trap capable of resolving piconewton (pN) forces, Åmströngs (Å) distances and millisecond (ms) event times. The trap was calibrated as described in Bustamante and Smith[39], using a stiffness of 0.1 pN/nm. Individual MJ0366 molecules were attached to two polystyrene beads through modified 558 bp dsDNA linkers as shown in figure 5, where MJ0366 is tethered to them by means of disulfide bonds. The experiment consisted in stretching the protein from it ends at a constant velocity, 100 nm/s, by moving the trapped sphere in the optical trap away from the one fixed in the pipette. The applied force ranged from 5 to 30 pN. As explained, the tethered protein was pulled and relaxed by its N-and C-terminus to mechanically unfold and refold, respectively, while recording the force and trap position. Quantification of these forces is based on the conservation of the light momentum as explained by Smith et al. (2003)[40] and the trap position is determined by detecting the position of the bead in the PSD detector. This was done without BiP in the optical tweezers buffer and with 1µM BiP present in solution with different concentrations of ATP (2 mM, 0.33 mM, 0.1 µM) or ADP (2 mM), or with control proteins, 1 µM lysozyme or 1 µM BSA. The experiments were carried out either until at least 100 pulling events to stretch and relax

the protein were recorded, or until the tether ruptured. In each experimental condition data of at least three different pairs of beads was recorded.

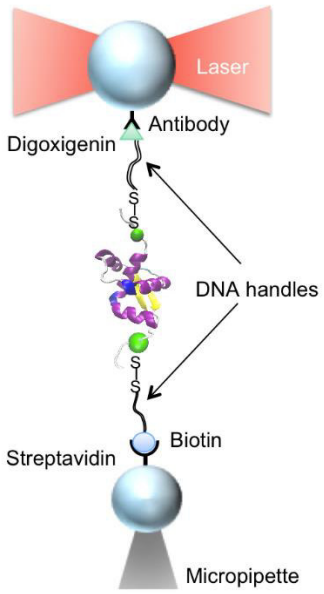

Figure 5. Experimental optical tweezer setup. The substrate protein MJ0336 is tethered between two dsDNA handles through disulfide bonds at its N and C terminus. These handles are modified in its 5' ends with digoxigenin and biotin to bind the respective polystyrene beads coated with anti-digoxigenin and streptavidin, respectively. The anti-digoxigenin bead is held in an optical trap and the streptavidin bead is attached to a micropipette by suction. Figure provided by Maira Rivera.

4.2.6 Optical tweezers data analysis. The force at which protein unfolding/refolding occurs was determined as well as the distance of this event. In order to determine the latter, the curve was adjusted to a line before and after the unfolding/refolding and the distance between these lines was determined.

4.2.7 Worm like chain fit. The equation of the worm like chain shows the dependence of the force on the extension of a flexible polymer in a thermal bath. A long polymer tends to contract as thermal forces try to randomize any alignment of its chain segments. This force has an entropic origin and its magnitude is given by[40]:

$$F = \frac{k_B T}{p}\left[\frac{1}{4}\left(1-\frac{x}{L_C}\right)^{-2} - \frac{1}{4} + \frac{x}{L_C}\right] \quad \text{(Equation 1)}$$

Where k_B is the Boltzman constant (pNnm/K), p is the persistent length of the chain (a value of 0.65 nm is used[41]); x is the end-to-end extension, Lc is the contour length; calculated by multiplying the number of amino acids by 0.36 nm/aa. The measured folded extension was subtracted from the contour length to determine the distance between the attachment points of the DNA handles in the absence of force. For each rip (sudden change in extension under application of force) for mechanical unfolding in the force-extension traces, the length of the rip is determined and is placed on a scatter plot of the rip length versus force. A best fit to the worm like chain values is made from these data by using the "Tweezer Analysis" program.

The theoretical contour length of a protein can be calculated according to the number of amino acids in its polypeptide chain, as explained before. This value should have a maximum limit corresponding to the number of amino acids between cysteines used to stretch the molecule. MJ0366 has 82 aminoacids tethered between the cysteines, between residue 6 and 89, so the maximum expected Lc value should be of 29.5 nm, but there are two factors to have into consideration. First, residues 6-11 and 87-89 are unstructured, so the rupture observed in the unfolding event corresponds to the loss of structure between residues 12-86, to obtain the real data then, it is necessary to make a correction. Second, MJ0366 is a knotted protein, which contains a 3_1 knot in its structure. It has been observed that these knots when tightened generate a shortening of 4.7 nm in Lc[42]. Therefore, the actual theoretical Lc of MJ0366 is 24.8 nm.

4.2.8 Optical tweezers data processing. The data processing was performed with MATLAB using the "Tweezer Analysis" program, provide by Jesse Dill.

4.2.9 Quantification of total unfolding and refolding events. Pulling events with unfolding and refolding rips were clearly distinguishable from those without them, so the determination of a pulling event with or without rip was performed manually. The total number of pulling events refers to the number of cycles stretching and relaxing the protein. In figure 11A, shown later, there are 4 unfolding and 4 refolding cycles, which all exhibit unfolding and refolding

events. Therefore, the frequency for unfolding and refolding for this example is 100%. The four unfolding and refolding cycles shown in figure 11B exhibit only two unfolding events (pulling 1 and 7) and only one refolding event (pulling 8). The frequency of unfolding and refolding in this example is 50% and 25%, respectively. The entire statistics of this work includes around 300 unfolding and refolding cycles for each condition, which add up to a total number of 2491 unfolding and refolding traces. The errors for the frequencies of unfolding and refolding events due to the limited number of pulling cycles were calculated using the inverse beta function and a 95% confidence interval as in Puchner et al[43]. These errors mean that the true probability for the binomial unfolding and refolding distribution will be with 95% probability within the cited errors.

4.2.10 Determination of BiP's dissociation constants and kinetics. As shown in the results, the binding of BiP to the unfolded protein substrate can be detected by the loss of folding- and unfolding events following binding. Therefore, it is possible to calculate the dissociation constant K_D of BiP for the used substrate according to:

$$K_D = \frac{[S][BiP]}{[S:BiP]} = [BiP]\frac{P_{rip}}{P_{norip}} = [BiP]\frac{P_{rip}}{1-P_{rip}} \quad \text{(Equation 2)}$$

Where [S] is the concentration of the substrate protein, [BiP] is the concentration of BiP, [S:BiP] is the concentration of the BiP-substrate complex and P_{rip} and P_{norip} are the probabilities for observing rips and no rips. Again, the errors due to the limited statistics were calculated using the inverse beta function and a 95% confidence interval[43].

In the data, binding of BiP to the unfolded protein substrate is detected by a loss in re- and unfolding events and conversely unbinding of BiP is observed by the reappearance of re- and unfolding events. Therefore, it can be directly determined the time intervals that BiP stayed bound and unbound to the protein substrate and calculate the corresponding on- and off rates. By assuming a first order reaction for the on- and off times, the on- and off rate constants were calculated from the inverse average of the on- and off times. A first order reaction, which is modeled by an exponential distribution for the on- and off times, is a reaction that proceeds at a rate that depends linearly on only one reactant concentration, represented by A, where k is the rate constant and t is the absence or residence times of BiP.

First order reaction differential representation:

$$\frac{-d[A]}{dt} = k[A] \quad \text{Equation (3)}$$

First order reaction integral representation:

$$[A] = [A]_o e^{-kt} \quad \text{Equation (4)}$$

The mean for the probability density function for exponential distribution:

$$Mean(t) = \frac{1}{k} \quad \text{Equation (5)}$$

So the mean absence time (*at*) corresponds to the k_{off}^{-1} and the mean residence time (*rt*) corresponds to the k_{on}^{-1}:

$$Mean(at) = \frac{1}{k_{off}} \qquad Mean(rt) = \frac{1}{k_{on}} \quad \text{Equation (6 and 7)}$$

For each experimental condition, we determined the error of the average times due to the limited statistics by bootstrapping[44]: for each data set 10,000 random samples were drawn and from the resulting distribution of average times the variance was determined. This variance, which represents the uncertainty due to the limited statistics, was used as an error for on- and off times and the corresponding rates. The K_D was also calculated using these parameters:

$$K_D = \frac{k_{off}}{k_{on}} \quad \text{Equation (8)}$$

5. RESULTS

5.1. Specific objective 1

BiP has two domains, an ATPase domain, the nucleotide binding domain (NBD), and a substrate binding domain (SBD). The SBD, binds to polypeptides with diverse sequences, but most specifically it recognizes a heptameric motif, Hy(WX)HyXHyXHy, where Hy is a bulky aromatic or hydrophobic residue, W is tryptophan, and X is any amino acid[16]. Since BiP recognizes linear motifs enriched in hydrophobic residues, which due to their hydrophobic nature are most likely located in the interior of a folded protein, it has been proposed that BiP binds to the unfolded state of proteins. No direct observation of this has been carried out so far, as trying to unfold one protein while maintaining the folded functional structure of another it is quite difficult. The effect of traditional denaturing methods (chaotropic agents and temperature) are global and would affect both the same[27]. For this reason, force spectroscopy experiments using optical tweezers are ideal, as they act as local denaturing agents on the substrate of our choosing, MJ0366, without affecting BiP folding and function, thus being able to explore BiP's interaction with the different folding states of MJ0366.

5.1.1 BiP purification. Due to the high quantity of active protein required to perform the optical tweezers experiments a purification protocol was developed by combining and modifying two previously published protocols[33,34], as described in the material and methods section. The nickel affinity column purification yielded pure BiP protein (Fig. 6A Lane 9), but to further purify and remove inactive BiP this purification was followed by an ATP-agarose affinity column purification. With this protocol ~3 mg/L of purified BiP was obtained. All of the collected fractions during the purification procedure were assessed by a 10% SDS-PAGE (Fig. 6A).

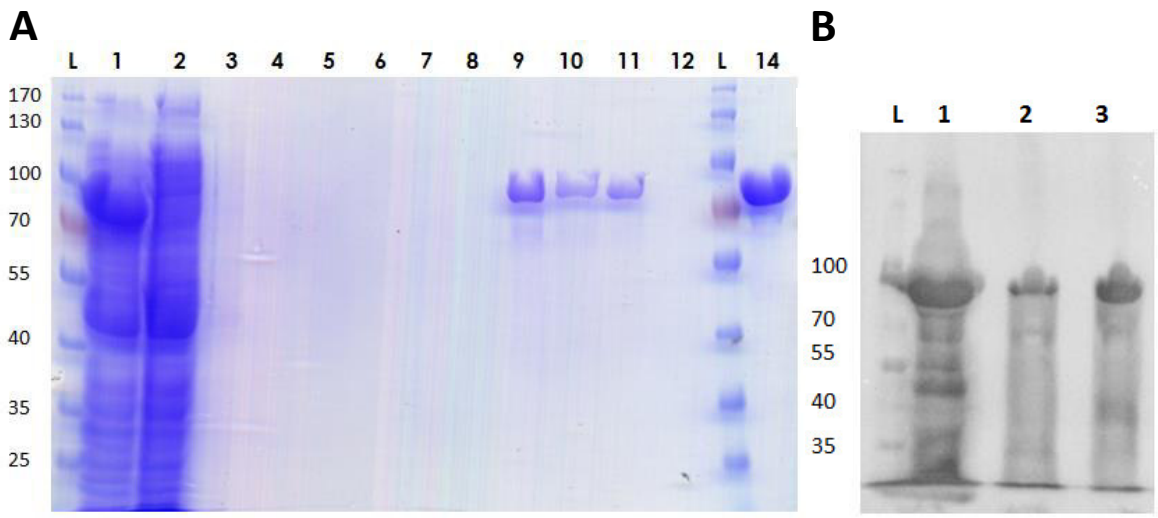

Figure 6. Purification of BiP chaperone. A. An SDS-PAGE 10% gel of collected fractions from every purification step. From left to right: Ladder (L), Supernatant (1), Flow through Nickel column (2), Wash 0 (3), Wash 1 (4), Wash 2 (5), Wash 3 (6), Wash 4 (7), Wash 5 (8), Peak Nickel column (9), Flow through ATP-agarose column (10), Wash Buffer C (11), Wash Buffer C + 1 M KCl (12), Ladder (L), Peak ATP-agarose column (14). **B.** Western Blot of supernatant (1), Peak Nickel column (2) and Peak ATP-agarose column (3). Purified BiP yeast protein is ~75 kDa. Ladder in kDa.

5.1.2 Coupled activity assay. BiP is an ATP dependent chaperone that hydrolyses ATP into ADP and Pi, so to confirm that purified BiP was active after the final purification steps an ATPase assay was needed. It was quickly noticed that BiP aggregated while performing spectrophotometrical coupled assay, so it was quite challenging to find an assay where BiP's activity could be measured without interference of BiP aggregates that dispersed light. Finally, a spectrophotometrical coupled assay measuring the formation of a formazan blue precipitate[36] at 550 nm was found to be the most effective. As figure 7 shows (green line), after an hour of reaction at room temperature in darkness, there is a signal peak around 550 nm, which indicates that formazan was formed. The pink line, a non-enzymatic control where reaction buffer was added instead of BiP, shows no signal at 550 nm. This results confirms that purified BiP is indeed active.

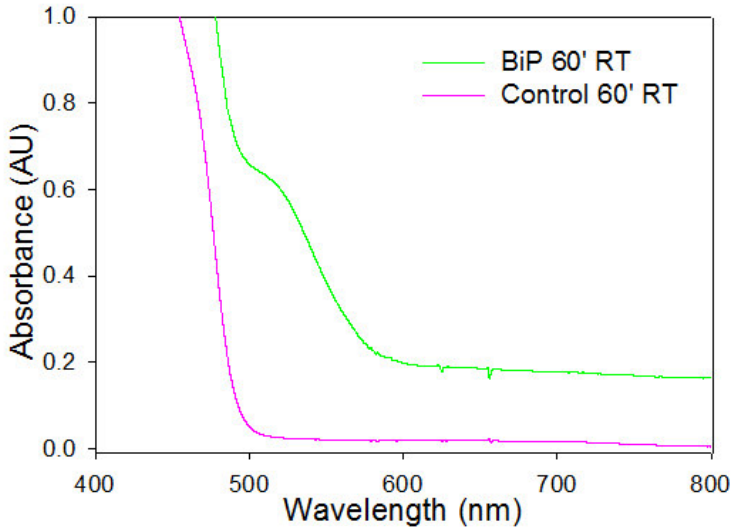

λ 550nm	0.21
[Formazan] µM	264
U	4.4 E-03

Figure 7. ATPase activity of purified BiP. Left: Formazan formation measured at 550nm after 1 hour of reaction at room temperature (RT) in the presence (green line) and absence (purple line) of BiP in solution. Right: Table that shows the absorbance measured at 550 nm after one hour of reaction, then the concentration of formazan calculated using the formazan extinction coefficient ($\varepsilon_{formazan}$), and finally the units of enzymatic activity obtained (µmol/min).

5.1.3 Choice of MJ0366 as BiP's protein substrate. MJ0366 is a knotted protein. Its mechanical unfolding and refolding behavior has been well characterized at single molecule level and exhibits clearly detectable folding and unfolding event (Fig. 10, shown later), which is crucial for this study [Doctoral Thesis Maira Rivera]. Furthermore, MJ0366 has most likely just one putative binding site for BiP, allowing a simpler analysis and interpretation of data. BiP binds to a hydrophobic motif, for this reason the protein substrate chosen to use in the experiments must have at least one probable motif in its sequence. To identify and determine the possible binding site of BiP in MJ0366 sequence first a hydrophobicity plot was built using the ProtScale bioinformatics resource from ExPASy. The hydrophobicity scale used was the Kyte-Doolittle scale[45]. This type of scales assigns a numerical value to each aa that defines their relative hydrophobicity. Figure 8 shows every individual value for each aa, the more positive the more hydrophobic it is. At MJ0366 C-terminus there is a hydrophobic region from aa 63 to 85 (Fig. 9A and B), and from aa 75 to 81 there is a sequence that perfectly fits the heptameric motif, ANLLLNA (Fig. 9C). In purple (Fig. 9A) are the sequences that somewhat fit the motif, but most likely with much less affinity, the first one has 5 hydrophobic aa but the 6 aa is the cysteine where the DNA handles are attached and they will probably interfere with BiP's binding. The second one has 4 hydrophobic aa but the other three in the motif are ones with a charged side chain and the motif does not have the best fit as the one proposed. The last purple region has several 7 aa sequences that have 4 or even 5 hydrophobic aa and somewhat fit the motif but they are all too close to each other, BiP has a 10-8 nm diameter in its open conformation[20] so it will bind to one of the motifs in that region.

Arg:	-4.5	Ser:	-0.8	Glu:	-3.5	Cys:	2.5
Lys:	-3.9	Thr:	-0.7	His:	-3.2	Phe:	2.8
Asn:	-3.5	Gly:	-0.4	Pro:	-1.6	Leu:	3.8
Asp:	-3.5	Ala:	1.8	Tyr:	-1.3	Val:	4.2
Gln:	-3.5	Met:	1.9	Trp:	-0.9	Ile:	4.5

Figure 8. Kyte-Doolittle hydrophobicity score table. Each aminoacid has been assigned a value. Hydrophobic residues have positive values and the hydrophilic residues have negative values[45].

A

MPLVGCMKEKKRATFYLYKNIDGRKLRYLLHKLENVENVDIDTLRRAIEA

EKKYKRSITLTEEEEVIIQRLGKSANLLLNAELVKLDECERENLYFQ

B

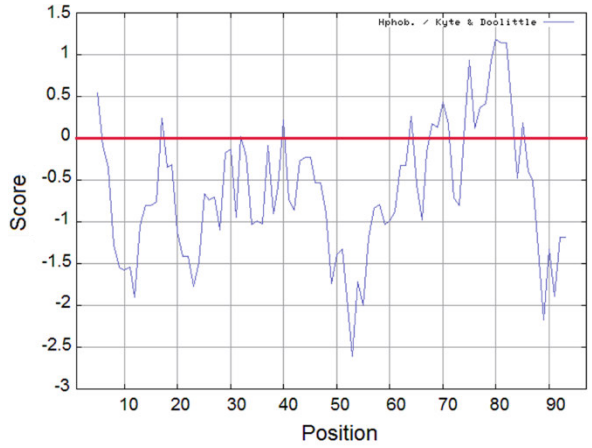

C

MJ0366 motif	**A**	**N**	**L**	**L**	**L**	**N**	**A**
Side chain charge	Hy	P	Hy	Hy	Hy	P	H
BiP binding motif	Hy	XW	Hy	Hy	Hy	X	Hy

Figure 9. Putative binding site of BiP in MJ0366 sequence. A. The highlighted blue region corresponds to the possible binding site, a region which has a high hydrophobicity and has the best fit with the BiP recognition motif Hy(WX)HyXHyXHy. The purple bands show other possible binding sites that fit in someway the motif. **B.** MJ0366 hydrophobicity profile. On the x-axis respresented is the amino acid sequence of MJ0366 protein and on the y-axis is the degree of hydrophobicity and hydrophilicity. The hydrophobicity scale used is the Kyte-Doolittle scale[45], over the red line regions with values above 0 are hydrophobic. **C.** How the chosen motif in MJ0366 fits the BiP's heptameric binding motif. Comparison between the first row is the chosen motif from MJ0366 sequence, the second row is the charge of each aminoacid and the third one is what type of aminoacid is expected in the motif. Hy is hydrophobic, P is polar, X is any type of aminoacid and W is tryptophan.

5.1.4 Robust detection of reversible MJ0336 unfolding and folding cycles in force-extension traces. The single molecule force spectroscopy experiments, using optical tweezers, consisted in the mechanical manipulation a protein from its ends at a constant velocity, 100 nm/s, to apply force as if it were a local denaturing agent. The experiment begins with a sole tethered construct in between the two polystyrene beads, the bead in the optical trap is separated from the one trapped in the pipette by suction at a constant speed. As represented in the force-extension curves (Fig. 10, shown later), the stretching of a protein first results in a rise in force caused by the entropic elasticity of the linker DNA molecules. Once the force is high enough to break the interactions that stabilize the native state, a protein domain or the entire protein unfolds, which results in a drop in force and in a sudden increase in the molecule's extension. If further stretched, the force again rises due to the combined entropic elasticity of the linker molecules and the unfolded polypeptide chain. Both the rupture force as well as the increase in contour length upon unfolding have characteristic values that depend on the energy barrier between the folded and unfolded state and the number of unfolded amino acids, respectively. Conversely, the refolding of a protein, which usually occurs at lower forces due to the non-equilibrium conditions of the experiment, results in an increase in the force and a decrease in the extension. As shown in figure 11A (shown later), we were able to perform multiple unfolding and refolding cycles with a single MJ0336 proteins with up to 100 repeats. In each cycle, the unfolding as well as refolding of MJ0336 resulted in a clear and quantifiable fingerprint with an average unfolding and refolding force of 19.5 ± 3.0 pN and 10.8 ± 0.9 pN respectively and a Lc of 25.4 ± 1.5 nm, which correlates with the theoretical value of 24.8 nm. Importantly, in all of the traces unfolding and refolding was observed, which demonstrates that the robust refolding of MJ0336 is detected with 100% efficiency (Fig. 11A, shown later). This experiment was performed without BiP in the system and 2 mM ATP, with a total of 5 molecules analyzed.

5.1.5 The chaperone BiP specifically binds to the unfolded substrate MJ0336 and inhibits its refolding. Having established a robust assay to observe reversible unfolding and refolding cycles of the protein substrate MJ0336, the effect of the chaperone BiP upon binding was investigated. In the presence of 1 µM BiP it was observed a diminution of the unfolding and refolding events (Fig. 10B and 11B), which is in contrast to experiments in the absence of BiP.

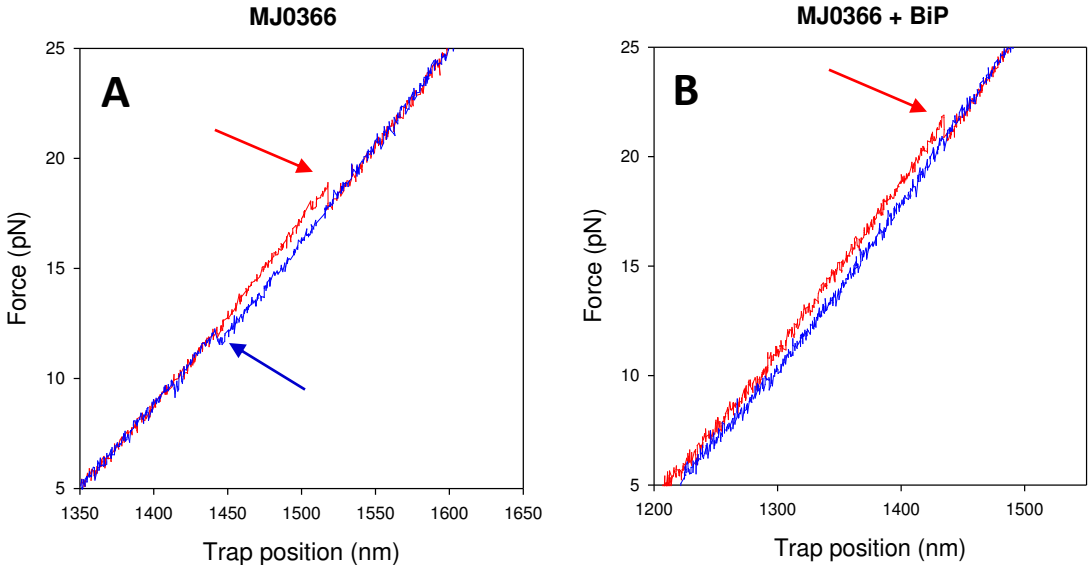

Figure 10. Force-extension curves of MJ0366 in absence and presence of BiP. A. Curve from pulling experiments at constant speed in buffer with 2 mM ATP**.** The red trace corresponds to MJ0366 stretching, where the force increases as the extension increases. The force indicated by the red arrow corresponds to the unfolding transition, what we here denominate an unfolding event. The blue trace corresponds to MJ0366 relaxing, where the force decreases as the extension decreases. The force indicated by the blue arrow corresponds to the refolding transition; the refolding event. **B.** Curve from pulling experiments at constant speed in buffer with 2 mM ATP and 1 µM BiP. The red curve shows the unfolding event indicated by the red arrow, but the blue curve does not show a refolding event.

Figure 11 shows force-extension curves spread in time (A and B) as an example of the effect of BiP binding, and how this affects MJ0366 folding (C). Figure 11A shows the robust reversible unfolding and refolding cycles. The molecules were subjected to these cycles up to 100 times or until the tether broke, and during all of this time not a single folding event was lost. In the presence of BiP (Fig. 11B), during these stretching and relaxing cycles to mechanically unfold and refold MJ0366 events were lost for periods of time. MJ0366 was initially able to unfold and refold, but at some point in the experiment folding events disappeared (traces 2-6) regaining them after a period of time (traces 7 and 8). The first event loss occurred after a successful unfolding event, as shown in Figure 11B (trace 2), meaning that the protein was able to unfold but not to refold. After this, the protein was not able to either unfold or refold during the stretching and relaxing cycles, until suddenly the events reappeared (trace 7). This loss of events for periods of time are due to the binding of BiP to MJ0366 (Fig. 11C), which has a probable binding site for BiP towards its C-terminal as shown in figure 9.

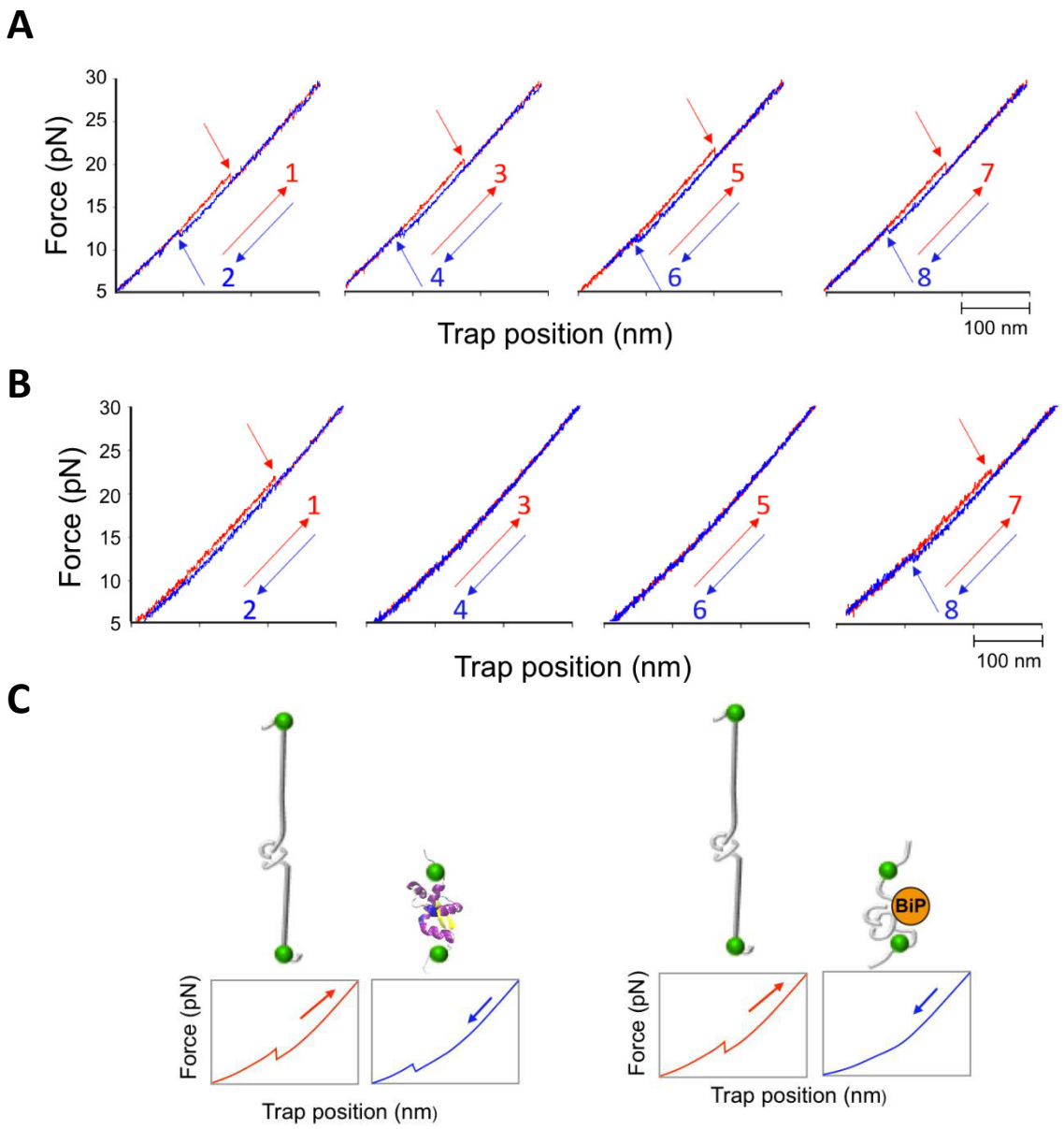

Figure 11. Effect of BiP binding on MJ0336 folding and unfolding. A. The force-extension curves showing the consecutive pulling cycles of MJ0336 at a constant speed of 100nm/s in the absence and **B.** presence of BiP. **C.** At the left, schematic representation of the mechanical unfolding and refolding of MJ0366, with their respective unfolding and refolding events. At the right, schematic representation of the mechanical unfolding and inhibition of refolding of MJ0366 due to the binding of BiP (orange) to the unfolded state, with their respective unfolding and lost refolding event. Pulling traces where unfolding occurs at high forces are shown in red and relaxation traces with refolding events at lower forces are shown in blue. In the upper pulling cycle the force spectroscopy experiments without BiP and with 2 mM ATP show that the pulling of the protein leads to its unfolding and later refolding in all cycles. In the lower pulling cycle, experiments were performed with 1 µM BiP and 2 mM ATP, and unfolding and refolding events were lost (second and third force-extension curves), and regained after some time (fourth force-extension curve).

Our results show that in the presence of BiP, the percentage of observable unfolding and refolding events during the stretching and relaxing of the protein was 76.6% and 70.9%, respectively (Fig. 12, Table 1). In table 2, the quantification of which folding event was first lost for every loss period, shows that from all the disappearances a 100% of the first losses was a refolding event (D.R and D.R% in table 2). The reappearance of the events was more variable, but usually the first observable event after a loss was unfolding event (R.U and R.U% in table 2). The average unfolding and refolding forces were not affected by presence of BiP (Fig. 13, Table 3).

In order to rule out unspecific effects of BiP the mechanical unfolding of MJ0366 was assayed in the presence of 1 µM lysozyme and 1 µM BSA, which do not have binding sites for MJ0336. With neither of these proteins unfolding or refolding events were lost (Fig. 12, Table 1) confirming that the interaction between BiP and MJ0336 is specific. In both control experiments, the unfolding forces were measured to be 16 ± 3 pN and 15 ± 2 pN, which agrees with the unfolding forces in the absence of protein in solution within the experimental error and the refolding forces remained the same (Fig. 13, Table 3).

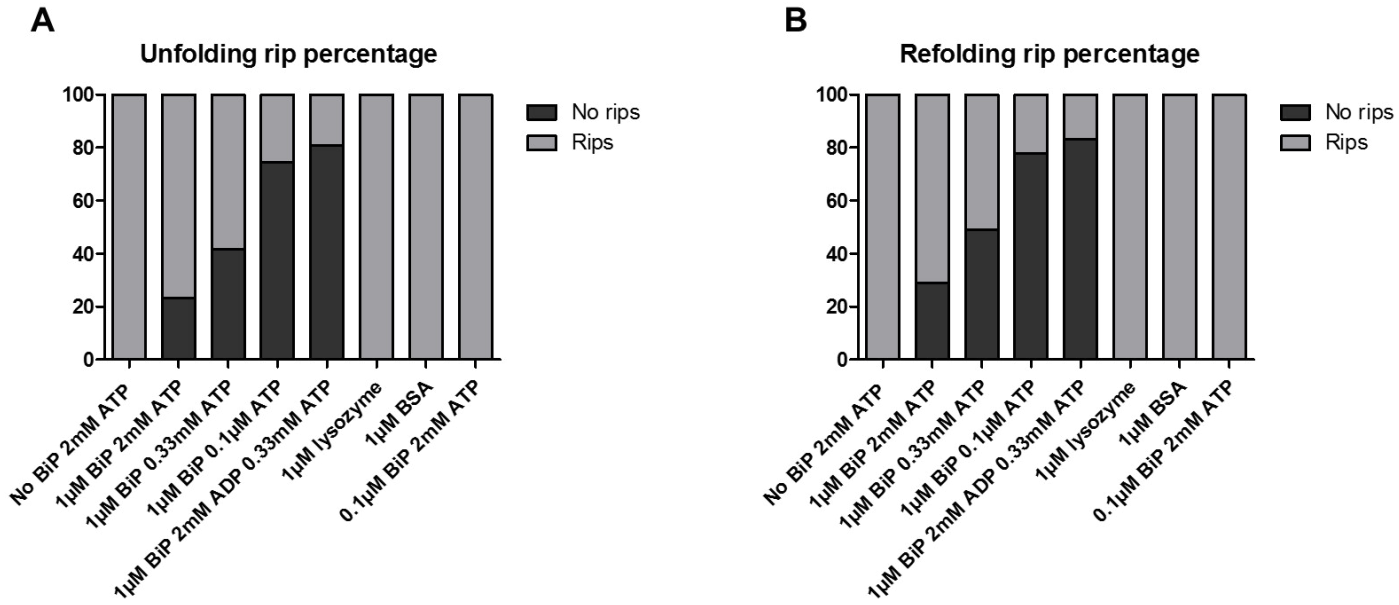

Figure 12. Frequency of unfolding and refolding events at different conditions. For all 8 conditions, the frequency of unfolding and refolding events were quantified, as well as the loss of these events. **A.** The frequency of unfolding and **B.** refolding events was compared at different buffer condition.

Table 1. Total amount of unfolding and refolding events.

Condition	Total events	Total events U[1]	U%	Total events R[2]	R%	N° of molcules
No BiP 2 mM ATP	344	344	100%	344	100%	5
1 µM BiP 2 mM ATP	342	262	76.6%	242	70.9%	8
1 µM BiP 0.33mM ATP	363	212	58.4%	185	51.0%	5
1 µM BiP 0.1 µM ATP	503	129	25.6%	111	22.1%	7
1 µM BiP 2 mM ADP 0.33 mM ATP	417	80	19.2%	70	16.8%	8
1 µM lysozyme	225	225	100%	225	100%	4
1 µM BSA	102	102	100%	102	100%	2
0.1 µM BiP 2 mM ATP	195	195	100%	195	100%	4

[1]Total unfolding events. [2] Total refolding events.

Table 2. Disappearances and reappearances of unfolding and refolding events.

Condition	Total disapp.	D.U	%D.U	D.R	%D.R	Total reapp.	R.U	%R.U	R.R	%R.R
2 mM ATP	20	0	0%	20	100%	20	16	80%	4	20%
0.33 mM ATP	18	0	0%	18	100%	18	13	72.2%	5	27.8%
0.1 µM ATP	12	1	8.3%	11	91.7%	7	7	100%	0	0%
2 mM ADP 0.33 mM ATP	18	0	0%	18	100%	12	10	83.3%	2	16.7%

During these stretching and relaxing cycles to mechanically unfold and refold MJ0366 events were lost for periods of time due to the binding of BiP. The loss of events could begin either after a successful unfolding event, meaning that it was the later refolding event that disappeared (D.R), or the loss could happen after a successful refolding event, meaning that it was the later unfolding event that disappeared (D.U). The total amount of times that an event disappeared for the first time after a successful event was quantified, as well what type of event was loss first. The same was done for the reappearance of the rips, where after a period of loss the events could reappear while stretching or relaxing, meaning that first event to be observed after a period of loss could be either an unfolding (R.U) or refolding event (R.R), respectively.
All conditions with 1 µM BiP.

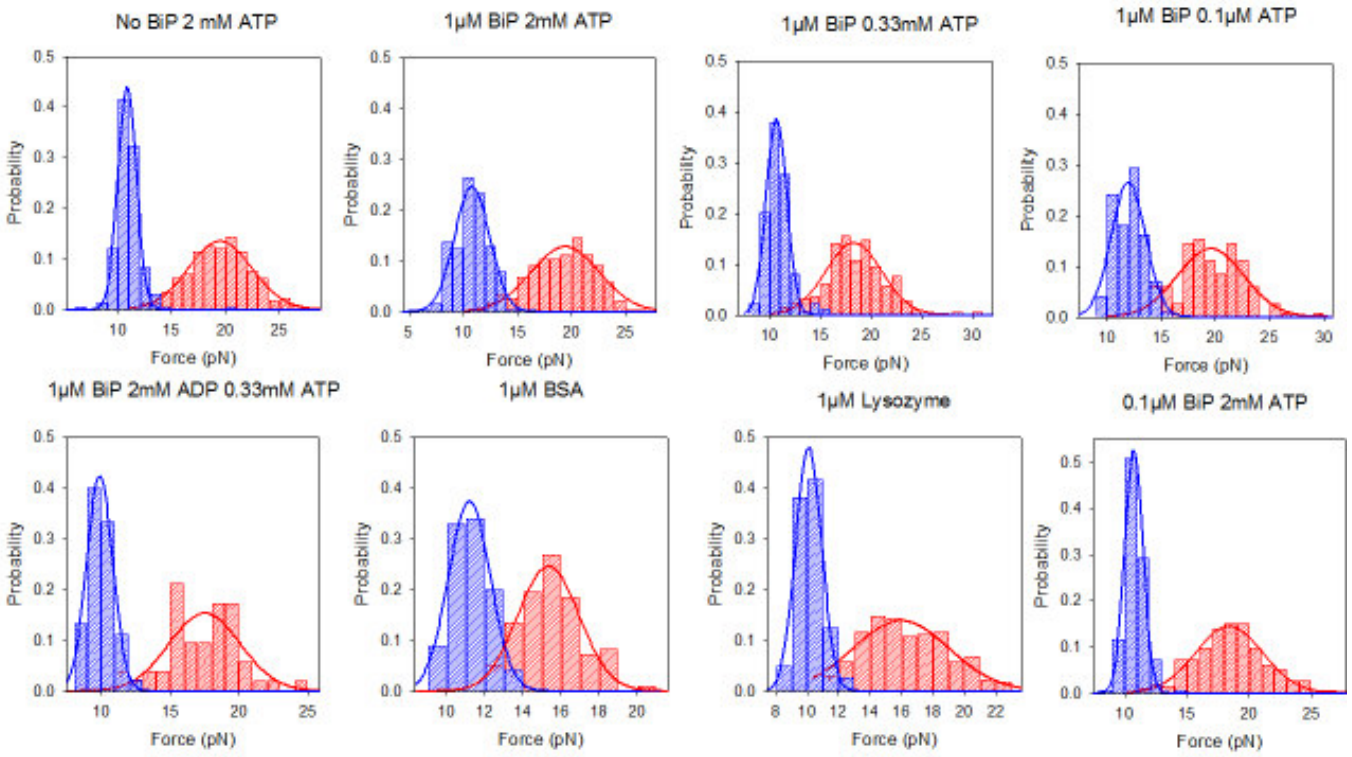

Figure 13. Unfolding and refolding force distributions of MJ0366. In red the histogram for unfolding forces, in blue the histogram for refolding forces. The distributions were fitted to a Gaussian function

Table 3. MJ0366 unfolding and refolding forces.

Condition	Unfolding force (pN)	Refolding force (pN)
No BiP 2 mM ATP	19.5 ± 3.0	10.8 ± 0.9
1 μM BiP 2 mM ATP	19.5 ± 3.2	10.8 ± 1.6
1 μM BiP 0.33 mM ATP	18.3 ± 2.8	10.7 ± 1.0
1 μM BiP 0.1 μM ATP	19.6 ± 3.1	11.9 ± 1.7
1 μM BiP 2 mM ADP 0.33 mM ATP	17.5 ± 2.8	9.9 ± 1.0
1 μM lysozyme	16.0 ± 3.1	10.1 ± 0.9
1 μM BSA	15.4 ± 1.6	11.2 ± 1.0
0.1 μM BiP 2 mM ATP	18.4 ± 2.7	10.7 ± 0.7

5.2. **Specific objective 2**

The function of BiP relies on cycles of ATP hydrolysis driving the binding and release of its substrate proteins. This cycle itself is an allosteric cycle, the nucleotide binding domain, NBD, regulates the affinity and kinetics of substrate binding in the substrate domain, SBD, and the binding of protein substrates stimulates the ATPase activity of the NBD. Binding of ATP to the NBD reduces the affinity of the SBD for protein substrates and binding of ADP increases the affinity[11,19]. Given this behavior characteristic of BiP, which extends to all HSP70 family members, the effect of these nucleotides at single molecule level was explored, as shown below.

5.2.1 BiP's dissociation kinetics is dependent on the type and concentration of nucleotides.

To investigate the effect of nucleotides on the affinity between BiP and MJ0366, decreasing concentrations of ATP were used (0.33 mM and 0.1 μM) beside the original concentration of 2 mM previously mentioned. The time that BiP remained bound to MJ0366 was reflected in the loss of refolding and unfolding events and was directly quantified from the extension vs. time traces. As the ATP concentration decreased (2 mM, 0.33 mM and 0.1 μM) BiP would stay bound to MJ0336 for longer periods of time (Table 4), which in turn lead to a decrease in the overall frequency of unfolding and refolding events (Fig. 12, Table 1, shown previously). Also, when 2 mM ADP was added to a solution with 1 μM BiP and 0.33 mM ATP as a competitor, BiP stayed bound to MJ0336 even longer (Table 4) and the loss of unfolding and refolding events was even greater (Fig. 12, Table 1, shown previously). The average unfolding and refolding forces were not affected by the concentration of nucleotides (Fig. 13, Table 3).

Table 4. Average absence and residence time of BiP.

Condition	Absence time (s)	Residence time (s)
1 μM BiP 2 mM ATP	86.55 ± 16.06	49.40 ± 8.03
1 μM BiP 0.33 mM ATP	79.77 ± 20.64	63.75 ± 17.48
1 μM BiP 0.1 μM ATP	36.73 ± 11.82	111.44 ± 35.40
1 μM BiP 2 mM ADP 0.33 mM ATP	37.85 ± 10.75	139.12 ± 43.64

Times were directly quantified from the extension vs. time traces. Absence and residence of BiP is reflected in the presence and absence of unfolding and refolding events, respectively.

It was further analyzed the binding and unbinding of BiP by assuming a first order reaction and by calculating the dissociation (k_{off}) and association (k_{on}) rates constants from the mean absence and residence times respectively, as explained in materials and methods. Also, in all of these analyses it was assumed that MJ0366 has only one binding site for BiP. This has not been experimentally demonstrated yet, but the analyzes of the sequence and the exponential distribution of the residence times (Fig. 14) allow for the use of this simple model for now. BiP's absence (free in solution) and residence (bound to MJ0366) times for each condition correspond to the periods of time with and without events. The off rate k_{off} decreased with the decrease in ATP concentration, being its lowest in the presence with ADP (Table 5). Using the ratio between k_{off} and k_{on} the apparent K_D was calculated (Table 5), which confirmed that at lower concentrations of ATP or in the presence of ADP the affinity for the substrate protein increased. Also, it was able to calculate the apparent K_D (Table 5) from the unfolding and refolding event probabilities (Table 1).

Table 5. Kinetic parameters for BiP in different conditions

Condition	App K_D (μM)*	App K_D (μM)**	k_{on} ($\mu M^{-1}s^{-1}$)	k_{off} (s^{-1})
1μM BiP 2 mM ATP	3.37±0.70	1.75±0.43	0.012±0.0022	0.021±0.0034
1μM BiP 0.33 mM ATP	1.43±0.25	1.31±0.50	0.013±0.0035	0.017±0.0046
1μM BiP 0.1 μM ATP	0.35±0.06	0.33±0.15	0.030±0.0098	0.0099±0.0032
1μM BiP 2 mM ADP 0.33 mM ATP	0.24±0.05	0.28±0.12	0.029±0.0082	0.0080±0.0025

*K_D calculated with Equation 1.
**$K_D=k_{off}/k_{on}$, Equation 8.

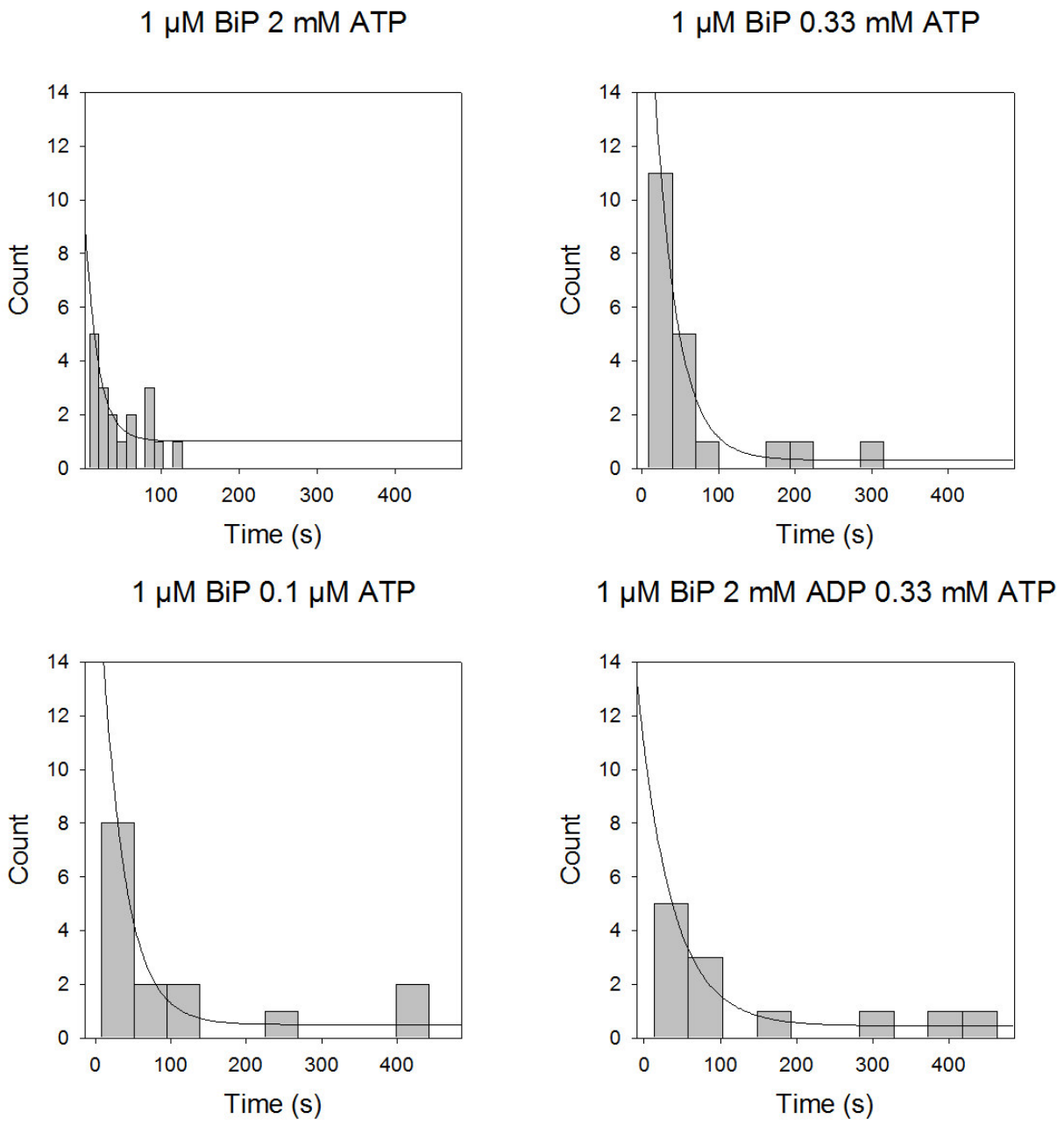

Figure 14. BiP residence time at different conditions. Residence was determined by the loss of unfolding and refolding events. Times were directly quantified from the extension vs. time traces.

6. DISCUSSION

It has been proposed that BiP binds to the unfolded state of proteins[16,26]. Studies have demonstrated that HSP70 recognizes hydrophobic motifs and that BiP specifically binds to a highly hydrophobic heptameric motif[16], which is most likely hidden in the core of the protein while folded and exposes when unfolded. For this reason, it may be logical to assume that chaperones bind to the unfolded state, but there are several intrinsically disordered proteins that expose hydrophobic patches[46], and it has not been demonstrated that BiP continuously binds to them on this patches. Also, BiP binds to folded proteins such as IRE1, an ER transmembrane protein[4]. Because of this, the assumption that BiP binds to the unfolded state cannot be generalized to all proteins, therefore it is important to experimentally prove this. Our results show that BiP indeed binds selectively to the unfolded state of proteins in a reversible manner, which is in agreement with its chaperone function. Furthermore, we were able to determine the affinity and kinetic rate constants of this process and how the type and concentration of nucleotides affected them.

6.1. BiP purification and aggregation

The purification protocol for BiP was set up to obtain high concentration of pure active BiP, as it was important for this experiments. Previous attempts to purify this protein from yeast using the ATP-agarose column or recombinant BiP from bacteria with only the nickel column yielded little amount of protein[33,34]. Using the two steps affinity column purification the yield was increased but the final concentration was not high enough. It was noted that the protocol was carried out in two different days, the first day the procedure was done until the nickel affinity column and the second day the pooled purified protein was passed through the ATP-agarose column. When this two steps were performed on a single day the concentration increased, but the total time of purification lengthened up to 12 hours of work at once, principally due to the imidazole gradient step, which was excessively long. Further studies showed that the gradient did not enhance the purification and so, it is not necessary for future purifications.

When a first coupled activity assay was performed, measuring the reduction of NAD^+ to NADH, it was observed that aggregates started to form as the absorbance signal saturated due to the light dispersion produced by the aggregate, masking the NADH signal at 340 nm. A discontinuous assay was tested, as well as measuring ATP conversion to ADP by capillary electrophoresis, both without success, as the aggregates were still a problem. Finally, the couple activity assay where formazan was measured as a final product was found to be the one where the aggregates did not bother the measurements. Although this is not the ideal assay, as a precipitate is formed, it is later shown by the effect of BiP in the optical tweezers experiment, the assay was appropriate enough to demonstrate that BiP was indeed active, but a better method is needed. This aggregation was also observed when ATP was attempted to be removed from purified BiP (BiP was finally eluted with a solution with 2 mM ATP), which made it difficult to eliminate the ATP to study the effect of BiP in the absence of nucleotides, so new conditions that maintain BiP soluble and active should be tested.

6.2. **Co-chaperones act together with BiP *in vivo* by stimulating ATP hydrolysis.**

BiP chaperone does not act alone, it interacts with co-chaperones and nucleotide exchange factors. The co-chaperones have a conserved domain known as J domain, that interacts with BiP, which stimulates its binding to peptides and also stimulates its ATPase activity[47]. These molecules have a biological relevance in BiP's function, but were chosen not to be used in this study. This was principally to keep the model simple, with more components it is more difficult to interpret what is specifically BiP's effect on the system and what is the effect of the other proteins. Also, studies by Misselwitz et al[47] show that the co-chaperones need to be in direct proximity to the substrate proteins to help deliver them to BiP and in our set up this was not possible, so it was decided that it was best to not use these other proteins and leave them for future studies.

6.3. BiP binds specifically to the unfolded state of MJ0366 and prevents protein refolding.

MJ0366 has clearly detectable unfolding and refolding events, meaning that the loss of these events after the addition of BiP to the system is due to BiP's binding to MJ0366. BiP, in its chaperone function, prevents the formation of tertiary contacts and refolding of the protein to its native state, which is confirmed by the fact that the loss of the events begun after a successful unfolding events. This effect was not permanent, as after some time the unfolding and refolding events reappeared, usually while stretching the protein to get it to unfold as shown in figure 11B, but this was variable, as the events sometimes reappeared while relaxing the protein. The control performed with lysozyme and BSA supports specific association of BiP with MJ0366, as neither of this proteins lead to the loss of events, not even BSA, a known sticky protein that has even been proved to have chaperone-like activity[48]. Also, the addition of BiP did not lead to any significant change in the unfolding and refolding forces. In previous studies with RNA hairpins it was found that binding of a protein to the folded hairpin lead to changes in the unfolding forces[49].

Therefore, with all of this information it can be concluded that BiP preferentially binds to the unfolded state of the protein substrate and inhibits the refolding of the protein substrate unfolded with optical tweezers. Our conclusion is consistent with the fact that BiP, as a chaperone, binds to unfolded proteins stabilizing their unfolded state until they spontaneously fold or passing the protein to another chaperone[26]. BiP binds to a heptameric motif of hydrophobic/aromatic aminoacids, which are most likely hidden while the MJ0366 is folded and are exposed once it unfolds. This allows BiP to interact with the substrate protein after the unfolding process and to hinder the formation of tertiary contacts (Fig. 15), which is thought to be its primary role as a chaperone.

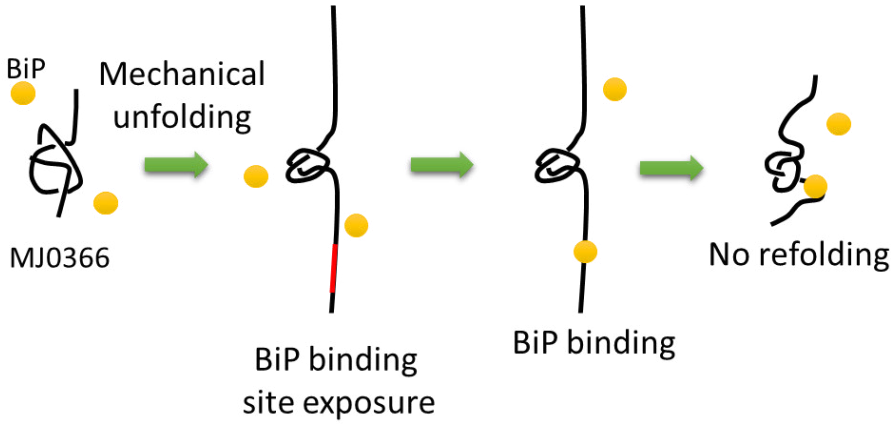

Figure 15. Model for substrate protein binding of BiP. MJ0366 in its folded state it free from BiP, as the binding site (red) is protected inside the protein hydrophobic core. After mechanical unfolding MJ0366 the binding site becomes exposed to the solvent where BiP is able to find it and bind, preventing protein refolding.

6.4. Optical tweezers set up and MJ0366 unfolding and refolding pattern allows for determination of kinetic parameters at single molecule level.

Not all proteins have a detectable refolding event, as some refold when there is no- or very low force affecting them. Some proteins even need some resting time at zero force for them to be able to refold. This is the case with MBP (Fig. 4), the substrate protein used by Bechluf et al[30] to study the chaperone function of SecB, and therefore prevented the authors to go further in their analysis and be able to calculate the affinity and kinetic parameters of this process. As previously stated, thanks to our set up and the detectable events of MJ0366, it was able to calculate the affinity and kinetic parameters of BiP binding to MJ0366 *in singulo*. Moreover, the K_D was able to be calculated through two different approaches, from the reason of k_{off} over k_{on} and from the unfolding and refolding event probabilities. Regarding the latter, it is the same to analyze a molecule ensemble at one determined time than to analyze one molecule over a period of time[50,51], so this experimental set up allowed to translate the concentration of components of the system into the probabilities of rips (P_{rip}) and probability of no rips (P_{norip}), which represent free substrate protein S in solution and S : BiP complex respectively, as shown in equation 2.

$$K_D = \frac{[S][BiP]}{[S:BiP]} = [BiP]\frac{P_{rip}}{P_{norip}} = [BiP]\frac{P_{rip}}{1-P_{rip}}$$

As shown in table 5, the K_D calculated with both methods resulted in very similar values, almost identical or within the same magnitude scale. This demonstrates that using either of these approaches leads to a correct determination of the dissociation constant and also shows that this set up allows for a robust determination of this constant, as long as the model protein being use has a visible unfolding and refolding event.

6.5. Nucleotide type and concentration affect BiP's affinity for MJ0366.

In bulk studies have shown the effect of the presence of ATP or ADP on the affinity of BiP for substrates[47]. In the presence of ATP BiP has a decreased affinity for its substrates, in comparison in the presence of ADP in the system. Structural studies of BiP with ATP or ADP bound to the NBD, have shown an allosteric cycle where the conformation of the NDB, determined by which nucleotide is bound to it. This affects the affinity and kinetics of the SBD[19] and how the binding of substrates affects the NBD in turn. In this study it was able directly observe BiP binding and release from a protein substrate and it also how these nucleotides and their concentration affected this process.

When the concentration of ATP was decreased the binding frequency of BiP increased, represented by the loss of folding events. The k_{on} for 2 mM and 0.33 mM ATP is the same, but when ATP is lowered to 0.1 μM or ADP is added, the k_{on} increases for both conditions in the same amount, meaning that the binding process is occurring faster than in the former conditions. For the k_{off}, there is a decreasing trend in this conditions, being almost the same as for 0.1 μM ATP and 2 mM ADP. The calculated K_D, by either approach, also shows a decreasing trend as ATP decreases or ADP is added, meaning that the affinity for the protein increased. At a single molecule level this shows that as we decrease the concentration of ATP, the conformational state of the SBD becomes more and more similar to the one of BiP with ADP bound to the NBD, which is supported by previous conformational studies by Marcinowsky et al.[29], using smFRET.

These changes in affinity evidence a direct relationship between the NBD and SBD, since the conformation that NDB adopts in the presence of a certain nucleotide leads to a conformational change in the SBD that affects its affinity for the substrate protein. Taken together this data shows at a single molecule level that the affinity between BiP and MJ0336 changes with different types of nucleotides and their concentration.

Through direct manipulation of a substrate protein of BiP we directly determined that this chaperone binds to the unfolded state of a protein, which other studies had indirectly shown but not directly proven as in this study. Using optical tweezers we were further able to measure the affinity, association and dissociation rate and compare the results with previous studies using smFRET[29].

6.6. Effect of multiple BiP binding sites and the force in the K_D

The calculated K_D is an apparent K_D, as it may be convoluted by 2 factors, the number of binding sites and the force. In our analyses a 1:1 stoichiometry was assumed between BiP and MJ0366 due to the sequence analysis previously mentioned in the result section and the exponential distribution obtained for the residence times. This model allowed us to generate equation 2 to calculate the apparent K_D, but to fully validate our calculations the real amount of binding sites for BiP must be experimentally determined. To do this a titration with BiP must be done using different concentrations. The simplest way would be to use the concentration that was determined as the apparent K_D in one of the conditions, for example in the condition with 2 mM ATP the apparent K_D using equation 2 is of 3.37 ± 0.70 μM. If MJ0366 has indeed just one binding site by using 3.37 μM BiP we should obtain 50% binding, meaning that we should get 50% of rips and 50% of rip loss.

$$3.37\mu M = \frac{[S][3.37]}{[S:BiP]} = [BiP]\frac{P_{rip}}{P_{norip}} = [3.37]\frac{50}{50}$$

If MJ0366 has more than one binding site this model would not fit our results, for example with 2 binding sites equation 2 would change as following:

$$K_D = \frac{[S][BiP]^2}{[S:2BiP]} = [BiP]^2 \frac{P_{rip}}{P_{norip}} = [BiP]^2 \frac{P_{rip}}{1-P_{rip}}$$

This change in equation 2 generates a significant difference in the expected result for the probability of rips, as shown by this example:

$$K_D = [BiP]\frac{P_{rip}}{1-P_{rip}} \qquad K_D = [BiP]\frac{P_{rip}}{1-P_{rip}} \qquad K_D = [BiP]\frac{P_{rip}}{1-P_{rip}}$$

$$4.07 = [1.6]\frac{P_{rip}}{1-P_{rip}} \qquad 3.37 = [1.6]\frac{P_{rip}}{1-P_{rip}} \qquad 2.67 = [1.6]\frac{P_{rip}}{1-P_{rip}}$$

$$P_{rip} = 0.72 \qquad P_{rip} = 0.68 \qquad P_{rip} = 0.63$$

Here are the probabilities for the mean app K_D for the condition of 1.6 μM BiP and 2 mM ATP was 3.37±0.70 (from 2.67 to 4.07).

The probability of rip if there were 2 binding sites according to equation 2 would be as following:

$$K_D = [BiP]^2 \frac{P_{rip}}{1-P_{rip}} \qquad K_D = [BiP]^2 \frac{P_{rip}}{1-P_{rip}} \qquad K_D = [BiP]^2 \frac{P_{rip}}{1-P_{rip}}$$

$$4.07 = [1.6]^2 \frac{P_{rip}}{1-P_{rip}} \qquad 3.37 = [1.6]^2 \frac{P_{rip}}{1-P_{rip}} \qquad 2.67 = [1.6]^2 \frac{P_{rip}}{1-P_{rip}}$$

$$P_{rip} = 0.61 \qquad P_{rip} = 0.57 \qquad P_{rip} = 0.51$$

Regarding the force, it is possible that BiP binds to its substrate protein depending on the stretching level of the polypeptide, meaning that there could be a force-dependence factor involved in BiP binding as well. To answer this, force clamp experiments could be done at high forces and observe if BiP still binds, but the problem is that MJ0366 has hopping at a very small range of forces, 12-15 pN, which are not high enough to test this. Structural studies by Yang et al[20] show that peptides bind to the SBD binding pocket extended, so this could support the idea that stretched linear sequences are the ones still able to bind to BiP, and so the force may not affect the binding. Another way to study this could be by using Dudko's analysis[52]. Dudko allows to obtain the rate (k) constants from a force histogram (Fig. 13) at different forces and from this, a graph of k versus force can be done. With this analysis it could be demonstrated if the force under which the protein is subjected to indeed affects BiP

binding, if there is no change the force is not a significant factor to take into consideration in our analysis.

7. CONCLUSIONS

1. BiP binds to the unfolded state of MJ0366 in a reversible manner, which is supported by the fact that the loss of events occurs after a successful unfolding event and that the unfolding and refolding forces do not change in the presence of BiP.

2. BiP's affinity is dependent on the type of nucleotide bound to the NBD and its concentration. ATP-NBD leads to a low affinity conformation of the SBD and ADP-NBD to a high affinity conformation.

3. Through single molecule force spectroscopy two different approaches (using the kinetic parameters and the probabilities) can be used to calculate the affinity constants.

8. FUTURE DIRECTIONS

MJ0366 is the simplest model that could have been used, as it has one probable binding site for BiP and has only one folding domain. This characterization of BiP binding/release from substrate proteins and the determination of its affinity and kinetic parameters gives rise to a platform to study diverse kinds of proteins. More complex proteins that have two or more folding domains or binding sites could be studied using this system, exploring in this way more complex folding pathways and how BiP participates in it. Preliminary studies with adenylate kinase, which has two folding domains, have shown that BiP does bind to it, and that after loss of events they never come back, showing a different behavior than with MJ0366.

Regarding future work with our current model, studies with different concentrations of BiP to confirm experimentally that there is only one binding site for BiP in MJ0366 will be performed. Also, using our current data the Dudko analysis will be done to determine if the force affects BiP's binding to MJ0366, as mentioned in the discussion.

REFERENCES.

1. Bartlett AI, Radford SE (2009) An expanding arsenal of experimental methods yields an explosion of insights into protein folding mechanisms. Nat. Struct. Mol. Biol. 16:582–588.

2. Hartl FU, Bracher A, Hayer-Hartl M (2011) Molecular chaperones in protein folding and proteostasis. Nature 475:324–332.

3. Mashaghi A, Kramer G, Lamb DC, Mayer MP, Tans SJ (2014) Chaperone action at the single-molecule level. Chem. Rev. 114:660–676.

4. Ron D, Walter P (2007) Signal integration in the endoplasmic reticulum unfolded protein response. Nat. Rev. Mol. Cell Biol. 8:519–529.

5. Saibil H (2013) Chaperone machines for protein folding, unfolding and disaggregation. Nat. Rev. Mol. Cell Biol. 14:630–642.

6. Bustamante CJ, Kaiser CM, Maillard RA, Goldman DH, Wilson CAM (2014) Mechanisms of cellular proteostasis: insights from single-molecule approaches. Annu. Rev. Biophys. 43:119–140.

7. Hartl FU (1996) Molecular chaperones in cellular protein folding. Nature 381:571–579.

8. Bukau B, Weissman J, Horwich A (2006) Molecular chaperones and protein quality control. Cell 125:443–451.

9. Beissinger M, Buchner J (1998) How chaperones fold proteins. Biol. Chem. 379:245–259.

10. Davis JE, Voisine C, Craig EA (1999) Intragenic suppressors of Hsp70 mutants: interplay between the ATPase- and peptide-binding domains. Proc. Natl. Acad. Sci. U. S. A. 96:9269–9276.

11. Kityk R, Kopp J, Sinning I, Mayer MP (2012) Structure and dynamics of the ATP-bound open conformation of Hsp70 chaperones. Mol. Cell 48:863–874.

12. Haas IG, Wabl M (1983) Immunoglobulin heavy chain binding protein. Nature 306:387–389.

13. Behnke J, Feige MJ, Hendershot LM (2015) BiP and its nucleotide exchange factors Grp170 and Sil1: mechanisms of action and biological functions. J. Mol. Biol. 427:1589–1608.

14. Gething MJ (1999) Role and regulation of the ER chaperone BiP. Semin. Cell Dev. Biol. 10:465–472.

15. Hendershot LM (2004) The ER function BiP is a master regulator of ER function. Mt. Sinai J. Med. N. Y. 71:289–297.

16. Blond-Elguindi S, Cwirla SE, Dower WJ, Lipshutz RJ, Sprang SR, Sambrook JF, Gething MJ (1993) Affinity panning of a library of peptides displayed on bacteriophages reveals the binding specificity of BiP. Cell 75:717–728.

17. Zhu X, Zhao X, Burkholder WF, Gragerov A, Ogata CM, Gottesman ME, Hendrickson WA (1996) Structural analysis of substrate binding by the molecular chaperone DnaK. Science 272:1606–1614.

18. McCarty JS, Buchberger A, Reinstein J, Bukau B (1995) The role of ATP in the functional cycle of the DnaK chaperone system. J. Mol. Biol. 249:126–137.

19. Zhuravleva A, Gierasch LM (2015) Substrate-binding domain conformational dynamics mediate Hsp70 allostery. Proc. Natl. Acad. Sci. 112:E2865–E2873.

20. Yang J, Nune M, Zong Y, Zhou L, Liu Q (2015) Close and Allosteric Opening of the Polypeptide-Binding Site in a Human Hsp70 Chaperone BiP. Struct. Lond. Engl. 1993 23:2191–2203.

21. Dill KA, Chan HS (1997) From Levinthal to pathways to funnels. Nat. Struct. Biol. 4:10–19.

22. Dobson CM, Šali A, Karplus M (1998) Protein Folding: A Perspective from Theory and Experiment. Angew. Chem. Int. Ed. 37:868–893.

23. Hartl FU, Hayer-Hartl M (2009) Converging concepts of protein folding in vitro and in vivo. Nat. Struct. Mol. Biol. 16:574–581.

24. Sharma SK, De los Rios P, Christen P, Lustig A, Goloubinoff P (2010) The kinetic parameters and energy cost of the Hsp70 chaperone as a polypeptide unfoldase. Nat. Chem. Biol. 6:914–920.

25. Frydman J (2001) Folding of newly translated proteins in vivo: the role of molecular chaperones. Annu. Rev. Biochem. 70:603–647.

26. Labriola CA, Giraldo AMV, Parodi AJ, Caramelo JJ (2011) Functional cooperation between BiP and calreticulin in the folding maturation of a glycoprotein in Trypanosoma cruzi. Mol. Biochem. Parasitol. 175:112–117.

27. Shank EA, Cecconi C, Dill JW, Marqusee S, Bustamante C (2010) The folding cooperativity of a protein is controlled by its chain topology. Nature 465:637–640.

28. Cecconi C, Shank EA, Dahlquist FW, Marqusee S, Bustamante C (2008) Protein-DNA chimeras for single molecule mechanical folding studies with the optical tweezers. Eur. Biophys. J. EBJ 37:729–738.

29. Marcinowski M, Höller M, Feige MJ, Baerend D, Lamb DC, Buchner J (2011) Substrate discrimination of the chaperone BiP by autonomous and cochaperone-regulated conformational transitions. Nat. Struct. Mol. Biol. 18:150–158.

30. Bechtluft P, Leeuwen RGH van, Tyreman M, Tomkiewicz D, Nouwen N, Tepper HL, Driessen AJM, Tans SJ (2007) Direct Observation of Chaperone-Induced Changes in a Protein Folding Pathway. Science 318:1458–1461.

31. Wang I, Chen S-Y, Hsu S-TD (2015) Unraveling the folding mechanism of the smallest knotted protein, MJ0366. J. Phys. Chem. B 119:4359–4370.

32. Vogel JP (1993) Kar2, the Yeast Homologue of Mammalian BiP/GRP78. Ph.D. Thesis. Princeton, NJ: Princeton University.

33. McClellan AJ, Endres JB, Vogel JP, Palazzi D, Rose MD, Brodsky JL (1998) Specific molecular chaperone interactions and an ATP-dependent conformational change are required during posttranslational protein translocation into the yeast ER. Mol. Biol. Cell 9:3533–3545.

34. Brodsky JL, Hamamoto S, Feldheim D, Schekman R (1993) Reconstitution of protein translocation from solubilized yeast membranes reveals topologically distinct roles for BiP and cytosolic Hsc70. J. Cell Biol. 120:95–102.

35. Bradford MM (1976) A rapid and sensitive method for the quantitation of microgram quantities of protein utilizing the principle of protein-dye binding. Anal. Biochem. 72:248–254.

36. Koga S, Yoshioka I, Sakuraba H, Takahashi M, Sakasegawa S, Shimizu S, Ohshima T (2000) Biochemical characterization, cloning, and sequencing of ADP-dependent (AMP-forming) glucokinase from two hyperthermophilic archaea, *Pyrococcus furiosus* and *Thermococcus litoralis*. J. Biochem.fig 128:1079–1085.

37. Christian AM. Wilson (2011) Single molecule studies by optical tweezers: Folding and unfolding of glucokinase from *Thermococcus litorali*. Ph.D. Thesis. Santiago de Chile, University of Chile.

38. Grassetti DR, Murray JF (1967) Determination of sulfhydryl groups with 2,2'- or 4,4'-dithiodipyridine. Arch. Biochem. Biophys. 119:41–49.

39. Bustamante C, Smith S (2005) Light-force sensor and method for measuring axial optical-trap forces from changes in light momentum along an optic axis. Available from: http://www.google.com/patents/US20050146718

40. Carlos Bustamante, Yann R. Chemla, Nancy R. Forde, Izhaky and D (2004) Mechanical Processes in Biochemistry. Annu. Rev. Biochem. 73:705–748.

41. Cecconi C, Shank EA, Bustamante C, Marqusee S (2005) Direct observation of the three-state folding of a single protein molecule. Science 309:2057–2060.

42. Dzubiella J (2009) Sequence-specific size, structure, and stability of tight protein knots. Biophys. J. 96:831–839.

43. Puchner EM, Alexandrovich A, Kho AL, Hensen U, Schäfer LV, Brandmeier B, Gräter F, Grubmüller H, Gaub HE, Gautel M (2008) Mechanoenzymatics of titin kinase. Proc. Natl. Acad. Sci. 105:13385–13390.

44. Efron B (1979) Bootstrap Methods: Another Look at the Jackknife. Ann. Stat. 7:1–26.

45. Kyte J, Doolittle RF (1982) A simple method for displaying the hydropathic character of a protein. J. Mol. Biol. 157:105–132.

46. Dunker AK, Silman I, Uversky VN, Sussman JL (2008) Function and structure of inherently disordered proteins. Curr. Opin. Struct. Biol. 18:756–764.

47. Misselwitz B, Staeck O, Rapoport TA (1998) J proteins catalytically activate Hsp70 molecules to trap a wide range of peptide sequences. Mol. Cell 2:593–603.

48. Finn TE, Nunez AC, Sunde M, Easterbrook-Smith SB (2012) Serum Albumin Prevents Protein Aggregation and Amyloid Formation and Retains Chaperone-like Activity in the Presence of Physiological Ligands. J. Biol. Chem. 287:21530–21540.

49. Cheng W, Arunajadai SG, Moffitt JR, Tinoco I, Bustamante C (2011) Single-base pair unwinding and asynchronous RNA release by the hepatitis C virus NS3 helicase. Science 333:1746–1749.

50. Tinoco I, Gonzalez RL (2011) Biological mechanisms, one molecule at a time. Genes Dev. 25:1205–1231.

51. Walters P (2000) An Introduction to Ergodic Theory. Springer Science & Business Media.

52. Dudko OK, Hummer G, Szabo A (2008) Theory, analysis, and interpretation of single-molecule force spectroscopy experiments. Proc. Natl. Acad. Sci. 105:15755–15760.